The Plant Cell, Vol. 26: 3964–3983, October 2014, www.plantcell.org

Jasmonoyl-L-Isoleucine Coordinates Metabolic Networks Required for Anthesis and Floral Attractant Emission in Wild Tobacco (*Nicotiana attenuata*)[C][W][OPEN]

Michael Stitz,[a] Markus Hartl,[a,1] Ian T. Baldwin,[a] and Emmanuel Gaquerel[a,b,2]

[a] Max Planck Institute for Chemical Ecology, Department of Molecular Ecology, 07745 Jena, Germany
[b] Centre for Organismal Studies, University of Heidelberg, 69120 Heidelberg, Germany

Jasmonic acid and its derivatives (jasmonates [JAs]) play central roles in floral development and maturation. The binding of jasmonoyl-L-isoleucine (JA-Ile) to the F-box of CORONATINE INSENSITIVE1 (COI1) is required for many JA-dependent physiological responses, but its role in anthesis and pollinator attraction traits remains largely unexplored. Here, we used the wild tobacco *Nicotiana attenuata*, which develops sympetalous flowers with complex pollination biology, to examine the coordinating function of JA homeostasis in the distinct metabolic processes that underlie flower maturation, opening, and advertisement to pollinators. From combined transcriptomic, targeted metabolic, and allometric analyses of transgenic *N. attenuata* plants for which signaling deficiencies were complemented with methyl jasmonate, JA-Ile, and its functional homolog, coronatine (COR), we demonstrate that (1) JA-Ile/COR-based signaling regulates corolla limb opening and a JA-negative feedback loop; (2) production of floral volatiles (night emissions of benzylacetone) and nectar requires JA-Ile/COR perception through COI1; and (3) limb expansion involves JA-Ile-induced changes in limb fresh mass and carbohydrate metabolism. These findings demonstrate a master regulatory function of the JA-Ile/COI1 duet for the main function of a sympetalous corolla, that of advertising for and rewarding pollinator services. Flower opening, by contrast, requires JA-Ile signaling-dependent changes in primary metabolism, which are not compromised in the *COI1*-silenced RNA interference line used in this study.

INTRODUCTION

In most angiosperms, floral development culminates with anthesis and stigma receptivity, the time in the flower maturation process at which sepals and petals of fertile flowers open to expose the reproductive inner organs to allow for pollination. Nonreproductive flower organs (Esau, 1977; Raven et al., 1986) also fulfill other crucial functions essential for plants' evolutionary success (Stanton et al., 1986; Nilsson, 1988). For instance, petals frequently play a dual role in protecting the valuable reproductive organs and providing the all-important advertising services required to ensure the optimal rate of successful outcrossed pollinations by producing a multitude of chemical and visual cues to attract animal pollinators, optimizing their behavior and minimizing the collateral damage that comes when these advertisements also attract florivores (Delph and Lively, 1989; Euler and Baldwin, 1996; Hoballah et al., 2007; Shang et al., 2011; Campbell et al., 2013). Unlike flower pigments, the synthesis of which usually occurs during early developmental stages, floral volatile and nectar production typically occurs after anthesis and is rapidly terminated after successful pollination (Drews et al., 1992; Jackson et al., 1992; Baldwin et al., 1997; Kessler et al., 2010). This coordination of corolla opening with the metabolic requirements of the production of pollinator advertisements and rewards is as important as the well-studied coordination of the optimal spatial arrangements of anthers and gynoecium in allowing flowers to successfully optimize their reproductive function (Reeves et al., 2012).

During flower maturation, the speed and rate at which floral organs elongate vary strongly with the flower's developmental stage (Smyth et al., 1990; Hill and Malmberg, 1991). Recent studies have shown that the developmental progression of distinct floral organs after organogenesis is controlled by the interaction of differing hormonal networks that vary in their dynamics (Chandler, 2010). In this respect, the complex molecular machineries that coordinate morphogenesis and tissue growth via the interaction of gibberellins (Koornneef and van der Veen, 1980; Hou et al., 2008), cytokinins (Huang et al., 2003), and auxins (Nagpal et al., 2005; Cheng et al., 2006) have been investigated extensively (Østergaard, 2009; Chandler, 2010). Others, such as abscisic acid (ABA), have received less attention, and few reports indicate an involvement of this phytohormone in the process of floral development (Weiss et al., 1995; Oliver et al., 2007). One prominent group of plant growth regulator compounds with fundamental functions in floral development consists of jasmonic acid and its derivatives, hereafter referred to as jasmonates (JAs). JAs occur ubiquitously in the plant kingdom

[1] Current address: IMBA, Dr. Bohr-Gasse 3, 1030 Vienna, Austria.
[2] Address correspondence to emmanuel.gaquerel@cos.uni-heidelberg.de.
The author responsible for distribution of materials integral to the findings presented in this article in accordance with the policy described in the Instructions for Authors (www.plantcell.org) is: Emmanuel Gaquerel (emmanuel.gaquerel@cos.uni-heidelberg.de).
[C] Some figures in this article are displayed in color online but in black and white in the print edition.
[W] Online version contains Web-only data.
[OPEN] Articles can be viewed online without a subscription.
www.plantcell.org/cgi/doi/10.1105/tpc.114.128165

and are known to regulate diverse processes ranging from root growth, anther dehiscence, and fruit ripening to plant defenses against insects and pathogens (Feys et al., 1994; Creelman and Mullet, 1995; Li et al., 2004; Wasternack, 2007; Wasternack et al., 2012). In response to stress or developmental cues, JA is synthesized from linolenic acid via several enzymatic reactions referred to as the octadecanoid pathway (Vick and Zimmerman, 1983; Blechert et al., 1995; Wasternack, 2007; Kallenbach et al., 2010). All genes encoding enzymes in this pathway, including phospholipase, lipoxygenase, allene oxide synthase (AOS), allene oxide cyclase (AOC), and 12-oxo-phytodieonic acid reductase (OPR), have been cloned from *Arabidopsis thaliana* and various other plants such as tomato (*Solanum lycopersicum*) and the wild tobacco *Nicotiana attenuata* (Schaller and Stintzi, 2009; Gfeller et al., 2010; Kallenbach et al., 2012). Previous work has shown that, in response to elicitation by biotic or abiotic stresses, JAs accumulate transiently in patterns that are regulated by several feedback loops (Paschold et al., 2008; Koo et al., 2011). By contrast, less is known about the regulation of JA biosynthesis in distinct floral tissues, although the existence of regulatory mechanisms differing from those reported in vegetative tissues has been suggested (Hause et al., 2000; Miersch et al., 2004).

Research with *Arabidopsis* mutants insensitive to coronatine (COR), a bacterial toxin and structural and functional analog of the phytohormone jasmonoyl-L-isoleucine (JA-Ile) (Staswick and Tiryaki, 2004), provided the first recognition of the role of JAs in floral development (Greulichi et al., 1995). Mutations at the CORONATINE INSENSITIVE1 (COI1) locus result in the production of flowers with nondehiscing anthers (Feys et al., 1994). Later studies identified the COI1 protein as the F-box component of an SCF-type E3-ubiquitin ligase complex (Xie et al., 1998) required for all JA-mediated responses examined to date. COI1 activity is mediated by the degradation of JASMONATE ZIM-DOMAIN (JAZ) proteins via the 26S proteasome (Chini et al., 2007, 2009; Thines et al., 2007; Y. Yan et al., 2007; Katsir et al., 2008; Fonseca et al., 2009; J. Yan et al., 2009), which in turn alleviates a negative transcriptional regulation of key MYB and basic helix-loop-helix transcription factors (Cheng et al., 2011; Qi et al., 2011; Song et al., 2011). Comparable roles for COI1 homologs in many other model plants have been confirmed (Li et al., 2004; Wang et al., 2005; Paschold et al., 2007; Ye et al., 2012). In several cases, such as the dehiscence of anthers or the growth of petals of *Arabidopsis* flowers, JA signaling has been shown to interact with other hormones such as auxins (Brioudes et al., 2009; Varaud et al., 2011; Cecchetti et al., 2013). In contrast with the JA-dependent regulation of male fecundity and petal growth in polypetalous plant species such as *Arabidopsis*, little is known about the role that JAs play in the timely development and opening process of functional petal complexes developed by sympetalous plants.

The developmental progression of floral tissues is tightly connected to fundamental changes in primary and secondary metabolism (Jackson et al., 1992; Dudareva et al., 2000). For instance, the rapid expansion of petal tissues is paralleled by a rapid increase in soluble sugar levels in many plant species (Evans and Reid, 1988; Bieleski, 1993; Vergauwen et al., 2000; Müller et al., 2010). The role played by carbohydrate metabolism in the coordination of developmental transitions and flowering time has recently received more attention (Cho et al., 2006; Wahl et al., 2013; Yang et al., 2013). Sugar and energy metabolism are thereby of central importance for the petals' osmotic pressure and energy-demanding processes that are required for anthesis and the expression of floral metabolic traits (Bieleski, 1993; Kuipef et al., 1995; Müller et al., 2010). While cross-regulation between carbohydrates and gibberellins during flower development has been established (Moalem-Beno et al., 1997), little is known about possible connections between floral carbohydrate metabolism and JA signaling, since most studies on JAs signaling metabolic output have been restricted to plant leaves and roots (Babst et al., 2005; Tejeda-Sartorius et al., 2008).

To understand the function of JA homeostatic regulation and signaling in coordinating flower development and the deployment of pollinator attraction traits, we analyzed flowers of *N. attenuata* transgenic lines in which either the JA flux was redirected or total JA biosynthesis or JA-Ile perception via COI1 was disrupted. Using a multidisciplinary approach, we demonstrate that the formation of functional corollas with completely opened limbs in *N. attenuata* is mediated by JA-Ile but is not impaired in the *COI1*-silenced RNA interference line used in this study. We further show that the rapid increases in corolla JA levels are developmentally regulated by a negative feedback mechanism requiring the interaction of JA-Ile with COI1, whereas the expression of floral pollinator attraction traits is positively regulated by this interaction. Finally, we provide concrete evidence for a connection between JA signaling and the regulation of energy metabolism in the expanding corolla limb, results that significantly expand our understanding of JA-mediated floral maturation processes.

RESULTS

Stepwise Interruptions in JA Signaling Have Organ-Specific Effects on the Maturation of *N. attenuata* Flowers

To investigate the role of JA biosynthesis and perception in floral development and anthesis through COI1, we examined a set of transgenic *N. attenuata* lines altered at different steps of the JA signaling pathway (Figure 1A). Total JA biosynthesis is interrupted in ir-*aoc* by silencing AOC (Schaller, 2001; Kallenbach et al., 2012), thereby preventing the formation of oxo-phytodieonic acid (OPDA), whose biological activity has been discussed recently (Goetz et al., 2012; Park et al., 2013). Ectopic expression of *Arabidopsis JASMONIC ACID METHYL TRANSFERASE* (*JMT*) and simultaneous silencing of *METHYL JASMONATE ESTERASE* (*MJE*) in *JMT/mje* redirects JA toward inactive methyl jasmonate (MeJA) and, conversely, reduces the formation of JA-Ile and other JA conjugates (Stitz et al., 2011b). Silencing *COI1*, on the other hand, interrupts JA-Ile perception through the F-box protein COI1 (Paschold et al., 2007).

From rigorous examinations of flower development in the glasshouse, we observed that ir-*aoc* plants produced flower corollas that are longer than wild-type corollas with limbs that failed to open completely (Figure 1B). ir-*aoc* styles were shorter than those of wild-type flowers, and anthers of this line show impaired dehiscence.

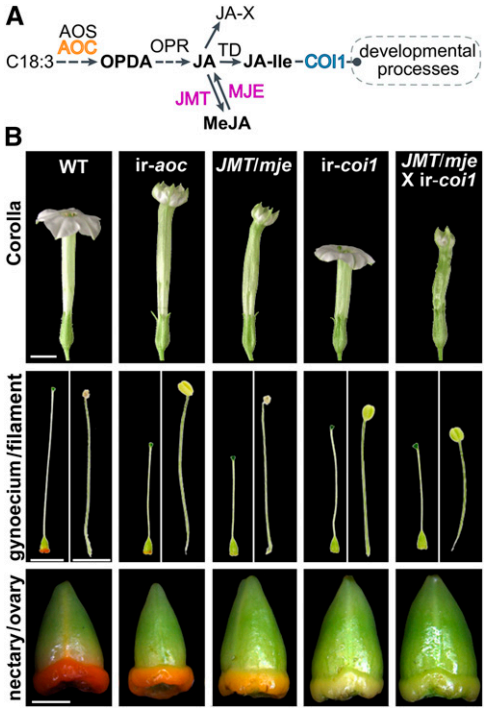

Figure 1. Floral Phenotypes of *N. attenuata* Wild-Type and Transgenic Plants Impaired in Different Steps of the JA Signaling Cascade.

(A) Simplified model of the JA pathway with emphasis on the sites of transgenic modifications used in this work. Silencing *AOC* (ir-*aoc*) interrupts JA biosynthesis at an early step before the formation of OPDA; ectopically expressing *Arabidopsis JMT* and simultaneously silencing *MJE* redirects JA toward inactive MeJA and abolishes the conjugation of JA to isoleucine; silencing *COI1* interrupts JA-Ile perception through the F-box protein COI1.

(B) The top row shows complete flowers of the wild type, ir-*aoc*, *JMT/mje*, ir-*coi1*, and a cross between *JMT/mje* and ir-*coi1* (*JMT/mje* × ir-*coi1*) at anthesis. Corresponding gynoecia (stigma, style, and nectary plus ovary) and stamens (filament with anther) are shown in the middle row, while the bottom row shows dissected nectaries at the base of the ovary. Each row of images was taken with the same magnification. Bars = 5 mm for corollas and gynoecia/filaments and 1 mm for nectaries/ovaries. [See online article for color version of this figure.]

Additionally, when compared with wild-type flowers, the nectary glands located at the base of the ir-*aoc* flowers displayed weaker pigmentation, which reflects defects in nectary maturation and nectar production. Like ir-*aoc*, *JMT/mje* corolla limbs also failed to expand completely, but style shortening and the juvenile character of nectary glands in *JMT/mje* were more pronounced, whereas corolla length and anther dehiscence were similar to those of the wild type. As reported previously in *N. attenuata* and other plant species, interrupting COI1-based JA perception caused severe impairments in anther dehiscence. Additionally, styles and corollas of ir-*coi1* were shorter than those of wild-type flowers. Strikingly, the limb expansion of ir-*coi1* flowers was not affected, whereas nectaries remained light green during the floral lifetime. *COI1* expression was strongly silenced in corolla (93.1%), nectary (92.3%), style (92.6%), and anther (81.6%) tissues (Supplemental Figure 1), and silencing efficiencies matched those reported previously for different ir-*coi1* plant tissues by Paschold et al. (2007). Hemizygous plants obtained by crossing *JMT/mje* and ir-*coi1* (*JMT/mje* × ir-*coi1*) recapitulated morphological alterations of *JMT/mje* plants to a stronger degree, except that anther dehiscence was additionally impaired (Figure 1B). These observations suggest that developmental alterations in floral development strongly depend on the nodes altered in the JA pathway.

JAs Control Synchrony and Velocity of Floral Organ Growth

We recorded the size of floral tissues dissected from individual buds developmentally determined by the length of their corolla (Figure 2A). Sepals elongated only marginally over the examined developmental frame, whereas corollas and filaments expanded synchronously until anthesis. Interestingly, we found that the growth of styles of the wild type and ir-*coi1* progressed linearly with corolla length, while style elongation in ir-*aoc* and *JMT/mje* was abruptly halted when the corolla reached ~13 mm. To determine the timing of JA regulatory functions over floral maturation, we defined a fixed range of sampling times, with the first day being defined as the day at which the corolla protruded from the sepals (1 DAP; Figure 2B, inset) and the day of anthesis (corolla limb fully expanded) as the final stage of our examinations. To clarify when alterations in the size and maturation of corollas were determined in transgenic plants, we examined the duration and daily increase in corolla length during the accelerated expansion phase until anthesis (Figure 2B). All monitored transgenic flower buds reached anthesis 1 d later than wild-type ones. While wild-type flowers characteristically remain open for 2 to 3 consecutive nights, flowers of transgenic plants typically wilted during the second night after anthesis.

Consistent with the above observations, relative elongation rates of corollas, filaments, and styles of individual flowers were consistently reduced, with the strongest effects detected for ir-*aoc* and *JMT/mje* style elongation (Supplemental Figure 2). Relative growth rate (RGR) calculations revealed that wild-type flower length increased exponentially for 2 d prior to anthesis, whereas all transgenic flowers showed an additional 1 d of exponential corolla elongation but had overall reduced RGRs compared with the wild type (Supplemental Figure 3). We collected corollas and examined whether total JA pool dynamics showed a similar delay to that observed for floral growth. Total JA accumulation peaked at 2 DAP in wild-type corolla tissues (Figure 2C) and then decreased sharply until anthesis (4 DAP), which strongly contrasted with the corolla tissues of ir-*aoc* plants, which accumulated ~120 times less JAs at the same DAP. However, while redirecting JA flux (*JMT/mje*) or impairing JA perception (ir-*coi1*) delayed the peaking time and altered the relative composition of JA pools, the overall magnitude of the accumulated JA pools was only marginally affected.

Transcriptional Activation of JA Biosynthesis Precedes JA-Ile Accumulation and Rapid Flower Maturation

From the above results, we inferred that a developmentally tuned elevation in the JA pathway flux was required during the initial phase of corolla elongation. To examine this inference, we

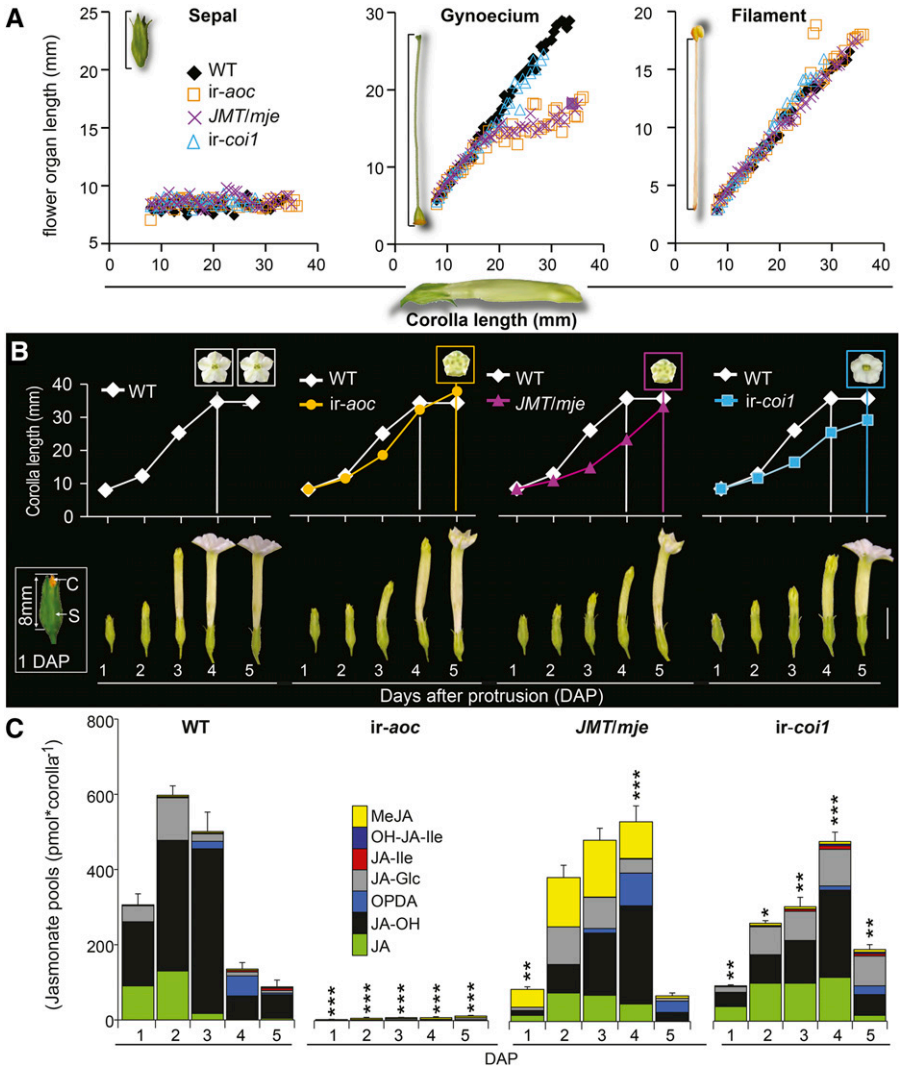

Figure 2. Altered Composition and Timing of JA Pool Accumulation Are Associated with Asynchrony in Organ Maturation and Delayed Anthesis.

(A) Scatterplots showing sepal, gynoecium, and filament lengths relative to the corolla length of individual flowers along floral maturation (complete flower size ranging from 7.8 to 38 mm).

(B) Mean ± SE (n = 5) corolla length measured every day (5:00 PM) from 1 DAP (white inset; C, corolla orange highlighted; S, sepal) until anthesis of transgenic flowers (5 DAP). Colored insets in graphs indicate time of corolla limb opening. Photographs in the bottom panel depict the degree of floral maturation over 5 d. Bar = 10 mm.

(C) Mean + SE (n = 3) summed levels of the six most abundant JAs detected at the indicated DAP in dissected corolla tissues of different genotypes: OPDA, JA, the sum of 12-OH-JA and 11-OH-JA (OH-JA), JA-Ile, JA-Glc, and MeJA. Asterisks denote significant differences between JA pool levels of wild-type and transgenic tissues at the same DAP in Bonferroni posthoc tests following a one-way ANOVA (***P < 0.000, **P < 0.001, *P < 0.05) after data were square root transformed.

quantified corolla transcript levels of central JA biosynthesis genes from 1 DAP until anthesis (Figures 3A and 3B). We additionally measured the transcript levels of *JAZd*, a recently identified transcriptional repressor of JA accumulation in complete *N. attenuata* flowers (Oh et al., 2013), and Na-*MYB305*, the *N. attenuata* homolog of *Arabidopsis MYB21*, a transcription factor in various plant species known for its role in floral development (Liu et al., 2009; Colquhoun et al., 2011; Reeves et al., 2012). Expression of the *N. attenuata* JA biosynthesis transcripts *AOS* (Kallenbach et al., 2012) and *THREONINE DEAMINASE* (*TD*) (Kang et al., 2006) peaked in wild-type, ir-*aoc*, and ir-*coi1* corollas at 1 DAP and decreased in conjunction with corolla expansion (Figure 3B). By contrast, the expression of *OPDA REDUCTASE* (*OPR3*) (Kallenbach et al., 2012), which is involved in JAZ biosynthesis, peaked at 2 DAP and remained low at other time points. Transcript accumulation of *TD*, which supplies Ile for JA-Ile formation, was impaired in ir-*aoc* and ir-*coi1* flowers at all developmental stages tested. *JAZd* levels exhibited a different

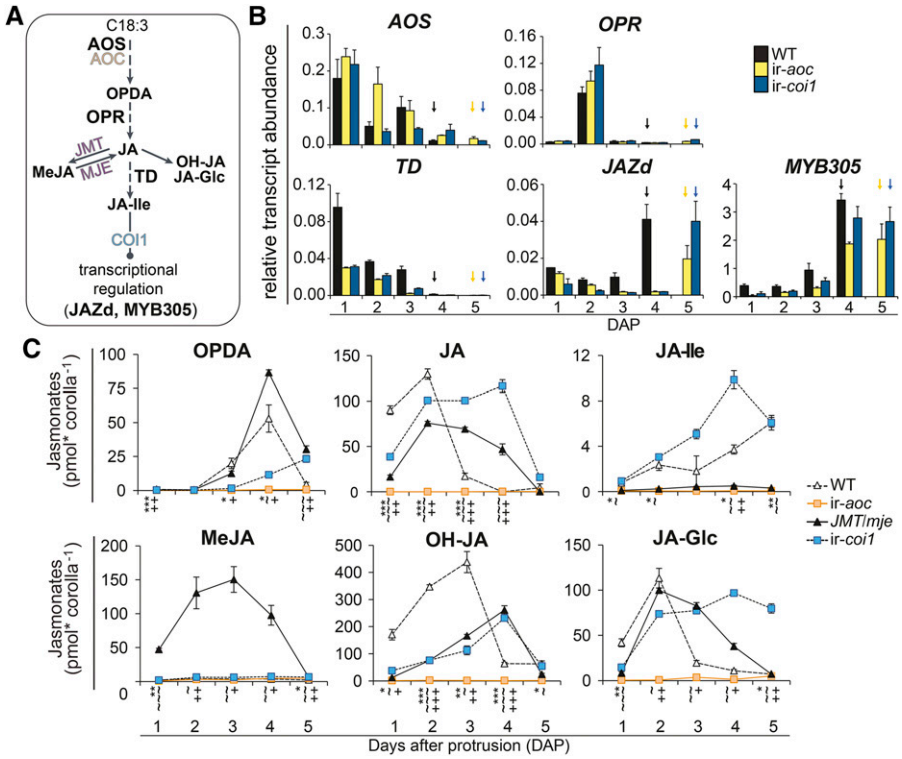

Figure 3. Transcriptional and Homeostatic Regulation of JA-Ile Levels during Corolla Maturation Is Deregulated in Transgenic Lines.

(A) Simplified model of the JA biosynthetic pathway highlighting genes analyzed by qRT-PCR.

(B) Mean + SE (n = 3) transcript abundance, relative to *EF1*α gene expression, of *AOS*, *OPR*, *TD*, *JAZd*, and *MYB305* in dissected corolla tissues during the expansion of wild type, ir-*aoc*, and ir-*coi1* flowers until the first day of anthesis (arrows).

(C) Levels of the six most abundant jasmonates (OPDA, JA, 12-OH-JA, JA-Ile, JA-Glc, and MeJA) as detected at the indicated DAP in corolla tissues of wild-type, ir-*aoc*, *JMT/mje*, and ir-*coi1* flower buds. Values are means ± SE (n = 3), and each replicate was obtained from 20+ pooled tissues of three plants. Asterisks (ir-*aoc*), tildes (*JMT/mje*), and plus signs (ir-*coi1*) indicate significant differences between tissues of wild-type and transgenic plants collected on the same DAP (unpaired t test; */~/+P < 0.05, **/~~/++P < 0.001, ***/~~~/+++P < 0.0001).

[See online article for color version of this figure.]

pattern, as its peak of expression matched each genotype's stage at anthesis, an accumulation dynamic that was also observed for *MYB305* (Figure 3B).

To visualize the impact of gene expression modulations on JA homeostasis, we analyzed individual JA dynamics during corolla elongation (Figure 3C). OPDA levels rose in the wild type until anthesis and then dropped rapidly, a pattern also observed in *JMT/mje* corollas, with the noticeable difference that OPDA peaking levels were ~30% higher than in the wild type and dropped before anthesis. In ir-*coi1*, the highest levels of OPDA were ~50% lower but, as in the wild type, peaked at anthesis. As expected, ir-*aoc* corolla tissues showed severe reductions in corolla OPDA (~98% less) and JA (~99% less) (Figure 3C). In wild-type corollas, JA peak levels at 2 DAP coincided with those of *OPR3* transcripts and total JA pools (Figures 3B and 3C). In line with the delayed maturation of these genotypes, JA accumulation in *JMT/mje* and ir-*coi1* corollas was shifted by 1 DAP. As expected, the reduction in JA levels in *JMT/mje* (~40% less than in the wild type) was mirrored by a massive MeJA accumulation absent in wild-type, ir-*aoc*, and ir-*coi1* corollas. Redirecting the JA flux toward MeJA in *JMT/mje* also translated into a dramatic reduction of JA-Ile levels similar to that observed in ir-*aoc* (~100 times lower than in the wild type) (Figure 3C). ir-*coi1* corollas showed a distinct pattern by constantly accumulating more JA-Ile, resulting in ~50% higher peak levels than in wild-type corollas. Accumulation of jasmonic acid-12-*O*-glucose (JA-Glc) followed that of JA, with the exception that in ir-*coi1* tissues, JA-Glc levels remained high until anthesis. In line with the JA dynamics, levels of inactive 11-hydroxy-jasmonic acid (11-OH-JA) and 12-OH-JA catabolites were temporarily shifted in all genotypes (Figure 3C).

Treatments with JA-Ile, MeJA, and COR Affect JA Fluxes and Restore Aberrant Patterns of Floral Development

To evaluate if alterations in the limb opening of ir-*aoc* and *JMT/mje* were directly caused by impaired JA-Ile accumulation, we conducted JA-Ile supplementation treatments and observed that exogenous applications of JA-Ile restored complete limb opening in ir-*aoc* and *JMT/mje* flowers (Figure 4A). We also conducted treatments with MeJA and COR (Figure 4B). Following demethylation by an MJE, MeJA can serve as precursor for JA-Ile formation in the wild type, ir-*aoc*, and ir-*coi1*. The bacterial

phytotoxin COR is a structural and functional homolog of JA-Ile that induces characteristic JA responses (Feys et al., 1994; Greulichi et al., 1995) and, due to its high bioactivity/permeability, is frequently used to investigate signaling functions of JA-Ile (Krumm et al., 1995). Neither MeJA nor COR treatments could restore the delay in anthesis of transgenic flowers (Supplemental Figure 4). We next assessed the effects of the treatments on the maturation of individual floral organs. COR treatments had a profound growth-promoting effect on the corolla length and fully restored limb expansion of ir-*aoc*, *JMT/mje*, and notably *JMT/mje* × ir-*coi1* flowers (Figures 4B and 4C). Backcrossing with wild-type plants did not change floral phenotypes of either *JMT/mje* or ir-*coi1* (Supplemental Figure 5). As expected, MeJA treatment rescued limb opening only of ir-*aoc* but not of *JMT/mje* or *JMT/mje* × ir-*coi1* corollas (Figures 4B and 4C). We observed similar COR and MeJA growth-promoting effects for style elongation, but neither styles of ir-*aoc* nor *JMT/mje*-treated flowers attained the size of wild-type flowers. None of the phenotypic alterations of ir-*coi1* flowers was significantly affected by the treatments (Figures 4B and 4C).

Striking differences were observed in the size and relative composition of corolla JA pools following complementation treatments (Supplemental Figure 6A). While increasing JA pool levels of transgenic flowers, MeJA treatment caused a slight reduction of maximal JA pools in the wild type. Strong reductions in JA pools after COR treatments were observed in wild-type as well as *JMT/mje* corollas collected prior to anthesis. Interestingly, this retroregulatory effect of JA-Ile/COR signaling over total JA accumulation did not affect the relative contribution of JA-Ile to wild-type JA pools or the expression of *TD* (Supplemental Figures 6B and 7) and was impaired in ir-*coi1* flowers. Shifted dynamics of JA-Ile and its catabolite OH-JA-Ile were observed compared with those of other JAs in the corollas

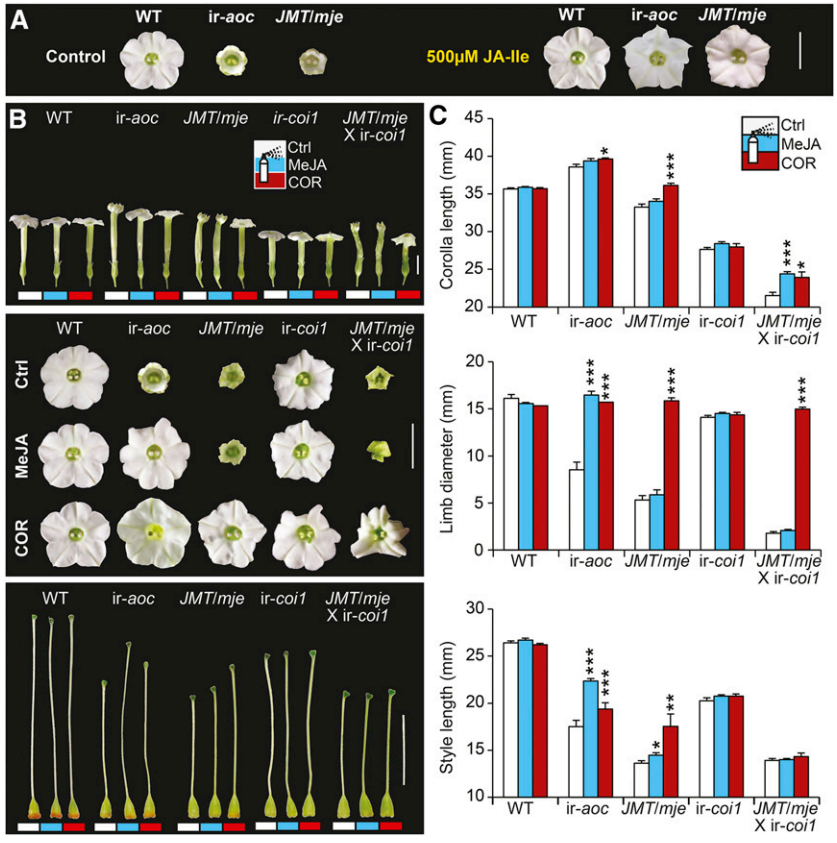

Figure 4. JA-Ile, MeJA, and COR Complementation Experiments Fully Rescue Limb Opening and Partially Rescue Style Elongation in JA-Deficient Flowers.

(A) Corolla limbs of the indicated genotypes after inflorescences were treated every other day with either control (0.02% Tween and 0.02% ethanol) or 500 μM JA-Ile solution. Bar = 10 mm.

(B) Photographs show complete flowers (top panel), corolla limbs (middle panel), and gynoecia (bottom panel) of the indicated genotypes. Inflorescences were treated every other day with either control (Ctrl; white bars), 100 μM MeJA (blue/light gray bars), or 1 μM COR (red/dark gray bars) solution. Bars = 10 mm.

(C) Elongation of corollas, corolla limb expansion, and length of corresponding gynoecia were monitored 10 d after the initial treatment and quantified for wild-type, ir-*aoc*, *JMT/mje*, ir-*coi1*, and *JMT/mje* × ir-*coi1* flowers (means + SE; $n = 15$). Asterisks indicate significant differences between control and MeJA- or COR-treated tissues of the same genotype (unpaired t test; *$P < 0.05$, **$P < 0.001$, ***$P < 0.0001$).

[See online article for color version of this figure.]

of nontreated ir-*coi1* flowers (Supplemental Figure 8), further suggesting a role for *COI1* in regulating JA-Ile metabolism.

Floral Sensitivity to COR-Mediated Limb Opening Is Restricted to the Initial Phase of Corolla Elongation

Transcriptional programs controlling flower maturation are activated early during morphogenesis (Reeves et al., 2012). To gain more insights into the timing of COR/JA-Ile signal transduction for limb opening, we assessed the latest developmental stage in which exogenously supplied JAs would trigger limb opening. Sensitivity assays conducted with complete inflorescences (Figure 5A) showed that only floral buds 9 mm or younger of JA-deficient plants (ir-*aoc*) responded to COR treatments and fully opened their limbs at anthesis. COR treatment of buds at later stages (>9 mm) failed to induce complete limb opening (Figure 5B).

Floral Nectar Secretion Requires COI1 Signaling and Is Partly Restored by COR Treatment in JA-Deficient Plants

Floral nectar volume is influenced by exogenous JA application (Radhika et al., 2010). Transcription factors of the R2R3-MYB family are known to be involved in stamen maturation (Dubos et al., 2010), and the function of MYB305 in modulating nectar secretion in ornamental tobacco (*Nicotiana tabacum*) has recently been described (Liu et al., 2009; Liu and Thornburg, 2012). Here, we investigated whether JA biosynthesis itself and/or signaling via COI1 were required for *N. attenuata* floral nectar secretion. Compared with the wild type, ir-*aoc* flowers secreted substantially less nectar, and no nectar was detected in ir-*coi1* (Figure 6A). COR treatments partly restored floral nectar secretion only in ir-*aoc* flowers, which strongly indicated that COI1 signaling is required for nectar secretion. To verify whether the restoration of nectar volume in ir-*aoc* translated from changes in transcriptional regulation, we measured the expression of nectar-related transcripts in nectary tissues (Figure 6B). ir-*aoc* nectaries had reduced transcript levels of β-*AMYLASE1*, the transcription factor *MYB305*, and the nectary-specific protein *NECTARIN1* (*NEC1* or *SWEET9*). These findings were consistent with the strong reduction of *MYB305* transcript levels in nectaries of untreated ir-*coi1* flowers, whereas *MYB305* expression in corolla, style, and anther tissues of this line was not significantly affected (Figure 3B; Supplemental Figure 9). However,

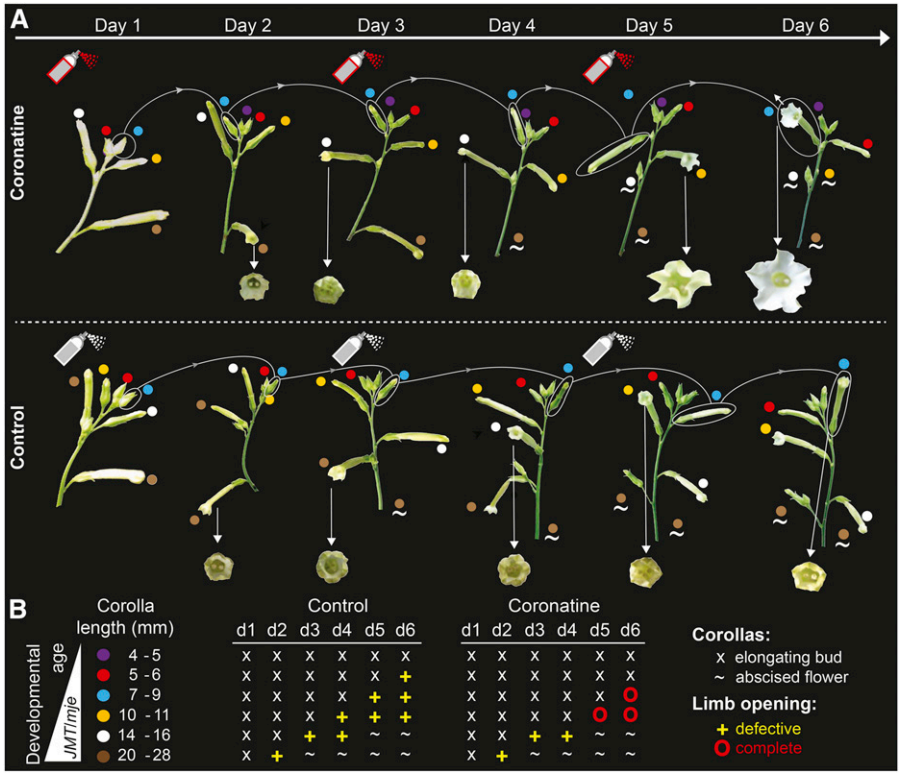

Figure 5. Complete Expansion of Corolla Limbs Requires COR/JA-Ile Signaling during Early Floral Bud Development.

(A) Photographs depict the development of two complete ir-*aoc* inflorescences over 6 d. On day 1 and every other day, intact inflorescences were treated with COR (top row) or a control solution (bottom row). Dots of the same color indicate the same floral bud in each image over the examined time frame. Arrows indicate corollas at anthesis, and tildes indicate abscised flowers. Photographs from one of two independent experiments with similar results are shown.

(B) Left, developmental age and size of individual buds present on the inflorescences before the initial treatments. Tables on the right indicate time after initial treatments and state of the single developing corollas, with x indicating expanding buds, + indicating defective limb opening, O indicating complete limb opening, and ~ indicating abscised flowers.

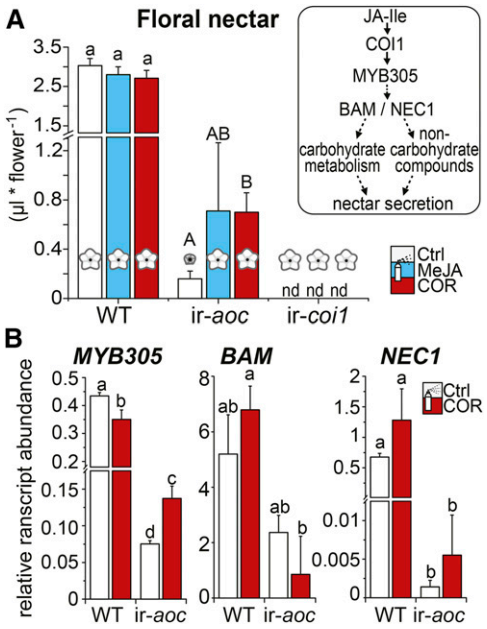

Figure 6. Expression of Nectar-Related Transcripts and Floral Nectar Secretion Are Compromised in JA-Deficient *N. attenuata* Flowers.

(A) Mean + SE (n = 11 to 18) nectar in flowers of plants that had been treated for 10 d every other day with control (Ctrl), 100 µM MeJA, or 1 µM COR solution. The box at right shows a schematic overview of transcriptional regulation during nectar secretion. A two-factor ANOVA with factor treatment and factor genotype revealed $F_{genotype}$ = 197.28 ($P < 0.000$), $F_{treatment}$ = 1.24 ($P = 0.29$), and $F_{treatment \times genotype}$ = 2.56 ($P < 0.039$). Different letters indicate significant differences in a Bonferroni-corrected posthoc test following a one-way ANOVA ($P < 0.05$).

(B) Transcript abundance (relative to *EF1*α gene expression) of floral nectar-related genes for the transcription factor *MYB305*, β-*AMYLASE* (*BAM*), and *NEC1* measured in nectary tissues of wild-type and ir-*aoc* flowers collected on the day of anthesis (means + SE; n = 3). Each replicate was obtained from 30+ pooled tissues of four plants. Different letters indicate significant differences in a Bonferroni-corrected posthoc test following a one-way ANOVA ($P < 0.05$).

[See online article for color version of this figure.]

COR treatment only partly restored the regulation of these transcripts in ir-*aoc* nectary tissues, a finding in agreement with the aforementioned changes in floral nectar volumes.

COI1-Dependent JA-Ile Signaling Regulates Upstream Steps in the Emission of the Floral Pollinator Attractant Benzylacetone

Typical *N. attenuata* flowers open at night and release benzylacetone (BA), which attracts night-active hawk moth pollinators for outcrossing (Euler and Baldwin, 1996; Kessler et al., 2008). Since the corolla limb is the main source for BA emissions (Euler and Baldwin, 1996), we assessed whether defective limb opening affected the emission of BA (Figure 7A). BA emissions in the headspace of JA-deficient flowers with defective limb opening (ir-*aoc*, *JMT/mje*) were substantially reduced compared with those of wild-type flowers. Reduced BA emission levels may be due to the reduced limb size of flowers produced by these genotypes. However, it is important to note that BA was also largely absent from the headspace of fully expanded ir-*coi1* flowers, indicating a strict dependency of BA emissions on JA-Ile/COI1-regulated metabolic processes rather than on the size of the emitting limb. To further support this conclusion, we measured BA levels in the headspace of MeJA- and COR-treated flowers. COR increased BA emission levels of ir-*aoc* and *JMT/mje* to those detected in the headspace of wild-type control flowers, while MeJA amplified BA release only in ir-*aoc* flowers. Consistent with earlier findings (Kessler et al., 2010), BA emissions were substantially lower during the second night of anthesis (Figure 7A, inset) and were similar among all groups.

The biosynthesis of BA is poorly understood other than that the activity of the polyketide synthase CHALCONE SYNTHASE1 (CHAL1) is required (Abe et al., 2001). To clarify whether alterations in BA emissions resulted from a deregulation in *CHAL1* expression, we measured *CHAL1* transcript abundance (Figure 7B). Importantly, maximal *CHAL1* expression in corolla tissues of all genotypes was detected in open flowers, irrespective of the treatments or the time required to attain anthesis. These results suggested that the complete opening of the limb alone is not sufficient for BA emission and requires intact COI1-dependent JA regulation of metabolic steps other than the expression of *CHAL1*.

Limb Opening Correlates with JA-Dependent Increases in Limb Fresh Mass and ABA Levels

To better understand the mechanisms behind corolla limb expansion, we monitored the opening process of single corollas of nocturnal wild-type and transgenic flowers (Figure 8A). Although ir-*aoc* and *JMT/mje* control flowers failed to expand their limbs to wild-type levels, the first phase of defective limb expansion in these two lines cooccurred with the complete opening of wild-type and ir-*coi1* limbs. MeJA and COR treatment did not affect the temporal dynamic of the limb-unfolding process in any of the tested genotypes, although they triggered a complete opening of ir-*aoc* and *JMT/mje* limbs.

In several species, anthesis coincides with rapid changes in petal fresh mass and osmotic potential, which correlate with dynamic reconfigurations of carbohydrate composition (Yap et al., 2008; Norikoshi et al., 2013). We quantified changes in limb fresh mass at the beginning and at the completion of anthesis (3 and 7:30 PM; Figure 8B). Wild-type (~9.9 mg) and ir-*coi1* (~9.4 mg) limb fresh mass did not differ at 3 PM and increased until anthesis to ~14.3 and ~12.7 mg, respectively. ir-*aoc* and *JMT/mje* limbs, by contrast, were substantially lighter than wild-type limbs at 3 PM (46 and 55%) and at 7:30 PM (36 and 47%). In agreement with the above observations, MeJA and COR (ir-*aoc*) or COR alone (*JMT/mje*) restored the limb fresh mass at both stages of anthesis.

It has been demonstrated previously that ABA is involved in the process of petal unfolding and BA emission (Koning, 1986; Ré et al., 2011). Accordingly, ABA levels measured at the beginning and at the completion of anthesis showed strong reductions, especially in dissected limbs of JA-deficient flowers (Figure 8B). MeJA (ir-*aoc*) and COR (ir-*aoc*, *JMT/mje*) treatments

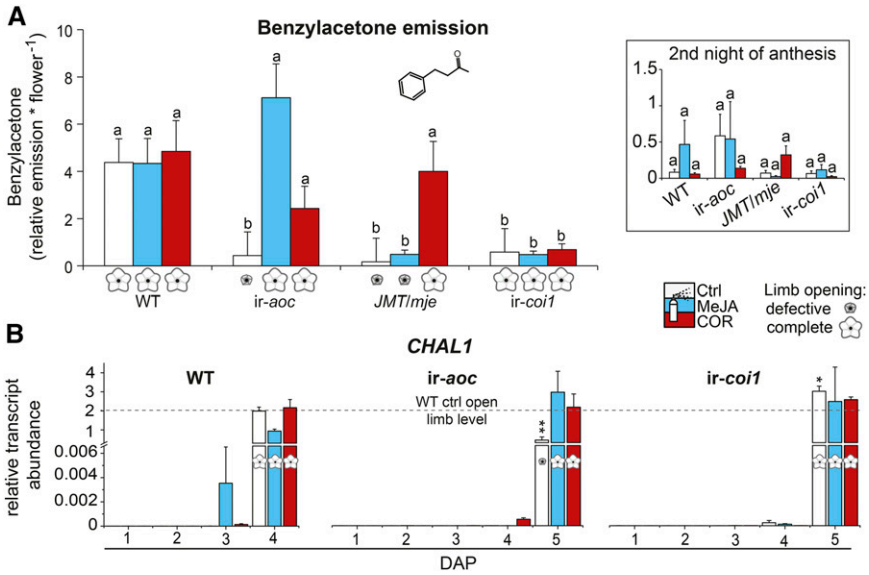

Figure 7. BA Emission and *CHAL1* Expression Are Differentially Affected in JA Biosynthesis/Perception-Deficient Flowers.

(A) Relative floral emission of BA (means + SE; $n = 11$ to 17) for wild-type, ir-*aoc*, *JMT/mje*, and ir-*coi1* flowers during the first night and the second night (inset) of anthesis. Buds of flowers monitored for BA emission had previously been treated every other day for 10 d with control (Ctrl), 100 μM MeJA, or 1 μM COR solution. A two-factor ANOVA with factor treatment and factor genotype revealed significant effects: $F_{treatment} = 4.98$ ($P < 0.008$), $F_{genotype} = 22.68$ ($P < 0.000$), and $F_{treatment \times genotype} = 6.445$ ($P < 0.000$). Different letters indicate significant differences in a Bonferroni-corrected posthoc test following an ANOVA ($P < 0.05$).

(B) Transcript abundance (relative to *EF1*α gene expression) of *CHAL1* in dissected corolla tissues of wild-type, ir-*aoc*, and ir-*coi1* plants at the indicated DAP and treatments (means + SE; $n = 3$). Each replicate was obtained from 20+ pooled tissues of three plants. Asterisks represent significant differences between wild-type control (ctrl) and treated transgenic flowers at anthesis (unpaired *t* test; *$P < 0.05$, **$P < 0.001$).

[See online article for color version of this figure.]

largely could restore ABA levels in limbs of transgenic plants, and similar results obtained for ABA measurements in complete corollas (Supplemental Figure 10) demonstrated a continuous increase in ABA levels until anthesis. The observation that the complementation treatments restore ABA in ir-*aoc* and *JMT/mje* corollas and limbs close to wild-type/ir-*coi1* levels prompted us to conduct an ABA supplementation treatment according to Ré et al. (2011). However, application of ABA failed to restore the limb opening of *JMT/mje* flowers (Supplemental Figure 11).

Limb Opening Is Associated with Global Changes in Carbohydrate and Energy Metabolism

Dynamic changes in carbohydrate metabolism during flower opening have been reported repeatedly in different plants (Evans and Reid, 1988; Ichimura et al., 2000; Yap et al., 2008; Norikoshi et al., 2013). In light of the pronounced developmental effects seen after COR treatments, we conducted a microarray experiment to identify genes coding for biological processes differentially regulated after COR treatment of ir-*aoc* flowers (Supplemental Figures 12 and 13). Among the 297 upregulated and 51 downregulated genes by COR, many were, as expected, related to auxin/jasmonate signaling or cell wall modification. A larger group, though, was assigned to carbohydrate/energy metabolism and glycolysis. Genes differentially regulated by the COR treatment in ir-*aoc* corollas are summarized in Supplemental Data Set 1A. This data set also mentions differentially regulated genes being directly homologous to known genes in *Arabidopsis* (Supplemental Data Set 1B).

Carbohydrates and especially intermediates of the tricarboxylic acid (TCA) cycle exert key regulatory functions for the osmotic potential and turgidity of plant cells (Evans and Reid, 1988; Fernie and Martinoia, 2009). We investigated the dynamics of limb carbohydrate and energy metabolism before and after corolla opening and detected that several glycolysis substrates (fructose, glucose/hexoses) were significantly altered in closed limbs of ir-*aoc*, ir-*coi1*, and *JMT/mje* compared with the wild type (Figure 9). The levels of maltose, for instance, were reduced in limbs of all transgenic corollas. By contrast, levels of myoinositol and sucrose were increased, especially in *JMT/mje* and ir-*coi1*, suggesting either a greater sucrose transport into corollas of these transgenic plants or different levels of invertase activity compared with the wild type. Aromatic compounds were equally altered in all transgenic lines, as seen for caffeic acid (>90% less than in the wild type) (Supplemental Figures 14 to 16).

The TCA cycle is a central hub interconnected with numerous aspects of a plant's metabolism, and citrate has frequently been reported to act as a feedback regulator on its own flux (Miernyk and Randall, 1987; Popova and Pinheiro de Carvalho, 1998; Sweetlove et al., 2010). We found significantly higher citrate levels in closed limbs of ir-*aoc* (~100% increase compared with the wild type) and *JMT/mje* (~200%) flowers, which implied

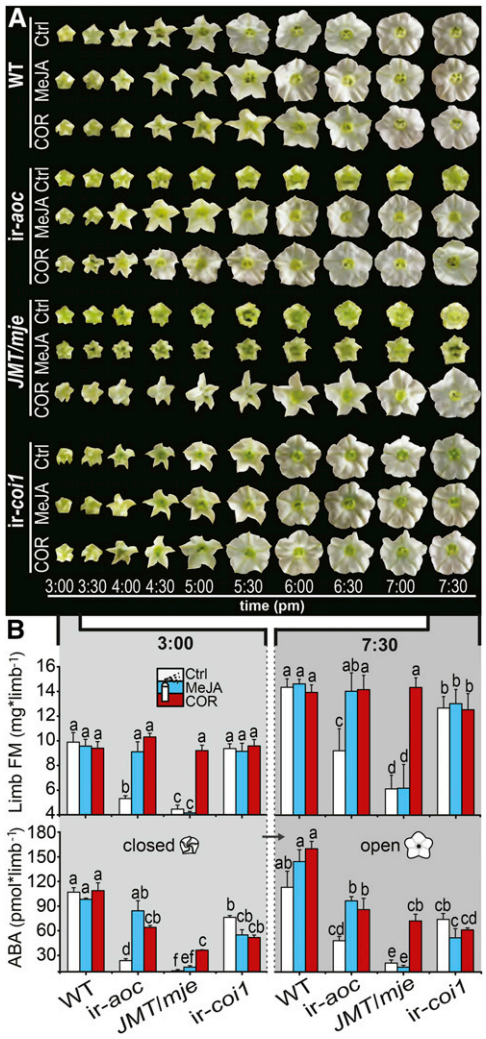

Figure 8. Rapid Changes in Limb Fresh Mass and ABA Levels during Anthesis Are Compromised in Transgenic Lines with Defective Limb Opening.

(A) Corolla limb expansion over time of characteristic single wild-type, ir-*aoc*, *JMT/mje*, and ir-*coi1* nocturnal flowers of inflorescences treated for 10 d every other day with control (Ctrl), MeJA, or COR solution.

(B) Fresh mass (FM; means + SE; $n = 3$ to 5) and ABA levels (means + SE; $n = 3$), with each replicate obtained from 20+ pooled tissues of three plants, of dissected corolla limbs measured prior to and after completion of anthesis (3:00 and 7:30 PM) of flowers that had been treated every other day for 10 d with control, 100 μM MeJA, or 1 μM COR solution. Two-factorial ANOVAs with factor treatment and factor genotype revealed significant effects for limb fresh mass (closed limbs: $F_{treatment} = 67.25$ [$P < 0.000$], $F_{genotype} = 97.45$ [$P < 0.000$], and $F_{treatment \times genotype} = 34.84$ [$P < 0.000$]; open limbs: $F_{treatment} = 36.82$ [$P < 0.000$], $F_{genotype} = 55.75$ [$P < 0.000$], and $F_{treatment \times genotype} = 26.94$ [$P < 0.000$]) and ABA levels (closed limbs: $F_{treatment} = 6.43$ [$P < 0.006$], $F_{genotype} = 98.59$ [$P < 0.000$], and $F_{treatment \times genotype} = 9.35$ [$P < 0.000$]; open limbs: $F_{treatment} = 21.05$ [$P < 0.000$], $F_{genotype} = 74.43$ [$P < 0.000$], and $F_{treatment \times genotype} = 9.48$ [$P < 0.000$]). Different letters indicate significant differences in a Bonferroni-corrected posthoc test following an ANOVA ($P < 0.05$).

[See online article for color version of this figure.]

a possible feedback inhibition. Indeed, compared with the wild type, we observed reduced levels of intermediates of the TCA cycle in closed limbs of ir-*aoc*, *JMT/mje*, and ir-*coi1*, whereas the levels of other intermediates such as fumarate were higher than in the wild type. Among these intermediates, malate may be of particular importance for the expanding limb, due to its previously described role in regulating turgor and cell expansion (Martinoia et al., 2007; Fernie and Martinoia, 2009). Although COR and MeJA treatments had only limited effects on oxaloacetate, these treatments largely restored the levels of several metabolites, such as citrate, fumarate, and, in the case of COR application on *JMT/mje*, fructose (Supplemental Figure 15). Comprehensive descriptions of JA-Ile/COR regulatory functions over primary metabolism are presented in Supplemental Figures 14 and 15. Together, these results demonstrated a key role for JAs as signals in tuning the interconnected metabolic networks in expanding corolla limbs.

DISCUSSION

JAs are the jack of all trades in plant signaling, with key functions in the deployment of defense responses against herbivores and in regulating root elongation and flower development. In this study, we used a set of transgenic plants altered in distinct steps of the JA signaling cascade to examine the role of JAs in regulating the maturation and opening of the sympetalous flowers of *N. attenuata*. We demonstrate that synchronized floral organ maturation requires intact JA-Ile formation and is preceded by a rapid rise in JA levels regulated by complex transcriptional modulations activated prior to corolla exponential elongation. Consistent with a direct function of JA-Ile in *N. attenuata* pollination, expression of the main pollinator attractants, nectar secretion and BA emission, is severely compromised in JA-Ile and/or COI1 signaling-deficient lines. While the expression of *MYB305* in the nectaries is dependent on JA-Ile and COI1, the *MYB305* transcript levels rise continuously in the corollas of both JA-Ile and COI1 signaling-deficient lines. Finally, we show that JA-Ile is a key signal for ABA accumulation in corollas and the global shifts in limb metabolism, fresh mass, and complete opening during anthesis. Together, these data robustly demonstrate that the process of anthesis in sympetalous flowers depends on JA-Ile-mediated changes in limb carbohydrate and energy metabolism (Figure 10).

Synchrony of Organ Maturation and Limb Opening Requires JA-Ile Formation

Efficient fertilization requires in most flowering plants the formation of generative organs as well as the temporal coordination of petal/corolla, filament, and style development before the opening of mature flowers at anthesis. Several of these critical steps involve tight regulation by the JA pathway, but the identity of signals within this pathway and their tissue-specific dynamics are not fully understood (Feys et al., 1994; Xie et al., 1998; Sanders et al., 2000; Ishiguro et al., 2001; Brioudes et al., 2009). Here, we show that distinct genetic manipulations of the JA signaling cascade in sympetalous flowers of *N. attenuata* result in overlapping and distinct aberrations in flower organ development,

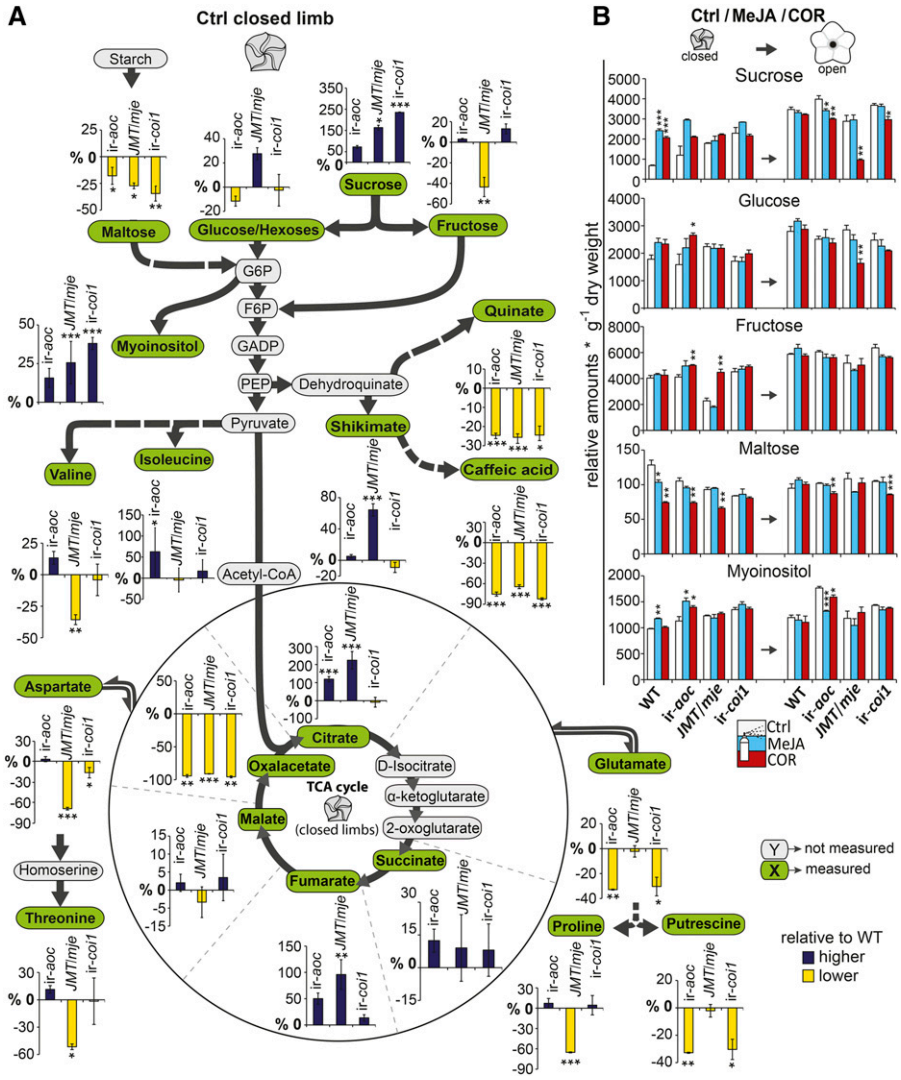

Figure 9. Accumulation of Carbohydrates and Intermediates in Energy Metabolism Is Impaired in Closed Limbs of JA-Deficient Flowers.

(A) Relative changes (%) in metabolite accumulation compared with the wild type as detected in closed corolla limbs before anthesis of control (Ctrl) and treated ir-*aoc*, *JMT*/*mje*, and ir-*coi1* flowers. Dark colored bars indicate higher levels than the wild type, and light/yellow colored bars indicate lower levels than the wild type. Asterisks indicate significant differences compared with wild-type levels (means ± SE; $n = 3$). Each replicate was obtained from 20+ pooled tissues of three plants. Glucose/Hexoses, combined glucose and hexoses; G6P, glucose 6-phosphate; F6P, fructose 6-phosphate; GADP, glyceraldehyde 3-phosphate; PEP, phospho*enol*pyruvate. Derivatized metabolic extracts were analyzed by two-dimensional gas chromatography coupled to mass spectrometry as described (Gaquerel et al., 2009). Asterisks denote significant differences between wild-type and transgenic tissues. **(B)** Relative sugar levels (means + SE; $n = 3$) were quantified at the beginning (closed) and after (open) completion of anthesis in control and MeJA- or COR-treated limb tissues. Asterisks indicate significant differences between COR- and MeJA-treated tissues versus control tissues of the same genotype (unpaired *t* test; *P < 0.05, **P < 0.001, ***P < 0.0001).

suggesting that different JAs have organ- and/or phase-specific developmental cue functions. For instance, style length was consistently reduced in all transgenic lines, whereas alterations in the length of corollas and filaments, anther dehiscence, and limb expansion varied greatly among the transgenic lines (Figure 4).

A framework for auxin and JA antagonistic signaling effects on petal growth was recently described in *Arabidopsis*, a plant producing flowers with polypetalous corollas. The current working model postulates that JA-induced expression of *BIGPETALp* (*BPEp*), a basic helix-loop-helix transcription factor preferentially expressed in petals, modulates petal size by restricting cell expansion (Szécsi et al., 2006; Brioudes et al., 2009). But the consequences of the JA depletion for corolla/petal expansion depend on where in JA biosynthesis/perception the alterations are made. Increases in sympetalous corolla length as seen in ir-*aoc* flowers are consistent with the increases in petal length of *Arabidopsis opr3* mutant plants, in which JA biosynthesis is interrupted downstream of OPDA formation (Brioudes et al., 2009). The other

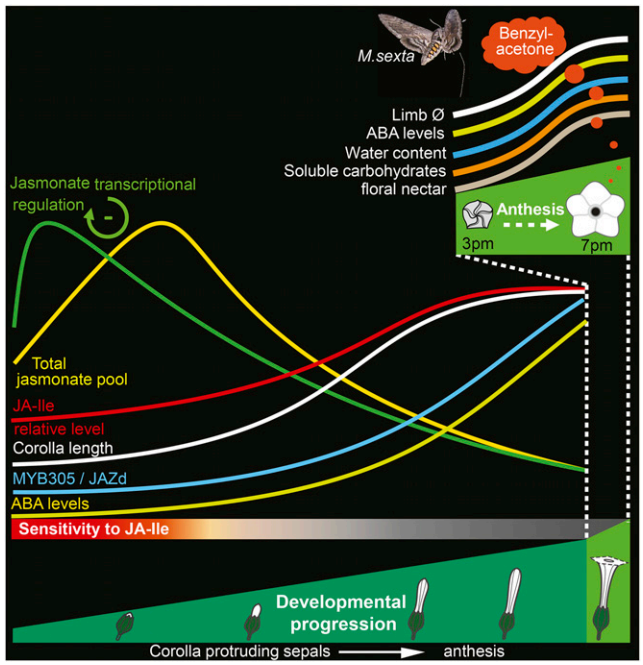

Figure 10. Model Summarizing JA Accumulation, Transcriptional Regulation, and Metabolic Processes Associated with Corolla Elongation and Limb Opening.

Fine-tuned JA-Ile signaling during early floral development controls *N. attenuata* corolla developmental progress and limb opening. Transcriptional and metabolite profiles highlight an early developmentally regulated burst in JA pools and further support a negative feedback function of JA-Ile/COR on JA biosynthesis. Increases in limb fresh mass, corolla transcript levels of *MYB305* and *JAZd*, ABA and soluble carbohydrate levels, and the subsequent complete limb expansion are not impaired in ir-*coi1*. However, signaling via the JA receptor COI1 is essential for BA emission and the expression of *MYB305* in floral nectaries. JA and COI1 mediate the regulation of nectary maturation and floral nectar secretion.

lines impaired in JA-Ile formation/perception either showed corollas as long as (*JMT/mje*) or shorter than (ir-*coi1*) those of the wild type. This suggests that metabolites synthesized downstream of AOC that are still produced in *JMT/mje* and ir-*coi1* genotypes may compensate for the growth-restricting function of JAs in the synergistic action of JA-Ile with AUXIN RESPONSE FACTOR8 (ARF8) and BPEp (Varaud et al., 2011). This inference is consistent with the observation that exogenous applications of MeJA or coronatine failed to restore corolla elongation of ir-*aoc* flowers to wild-type levels. Additional work indicates that *Arabidopsis* MYB24 and MYB25 may play more direct roles than BPEp in regulating petal elongation (Reeves et al., 2012). Consistent with this view, we observed a delay in the expression of *MYB305* in JA-deficient plants that paralleled that observed for the elongation of the corolla and the time needed to reach anthesis. However, we cannot rule out that alterations in our transgenic lines in the accumulation of other phytohormones such as auxin may have contributed to the observed phenotypes.

N. attenuata COI1-silenced flowers, like those of *Arabidopsis* (Feys et al., 1994) but in contrast with female-sterile tomato *coi1* mutants (Li et al., 2001, 2004), produce fertile pollen but are male-sterile due to impaired anther dehiscence (Paschold et al., 2007). As reported previously for singly transformed *N. attenuata JMT* plants, JA-Ile deficiency can additionally have an impact on fertility by decreasing style length and thereby separating the stigma from the anthers and decreasing self-pollinations (Stitz et al., 2011a). Notably, interrupting JA biosynthesis before OPDA formation in ir-*aoc* flowers caused both shortened styles and delayed anther dehiscence, thereby suggesting that intermediates of the JA pathway that are formed downstream of AOC and upstream of JA derivatization may act in the regulation of anther dehiscence.

Impairments in JA biosynthesis, but surprisingly not in COI1 signaling, cause a loss of the synchronous organ elongation that characterizes wild-type corollas and styles (Figure 2A), whereas anthesis was consistently delayed for 1 d (Figure 2B) in all transgenic lines due to severely reduced RGRs of corolla tissues during the exponential elongation phase (Supplemental Figure 3). The highest RGR coefficients in the wild type and the loss of synchronized corolla and style elongation in ir-*aoc* and *JMT/mje* (2 DAP) coincide with a rapid increase of JA pools in wild-type corollas (Figure 2C). This finding, together with the complete (limb) and partial (style) restorations observed after MeJA/COR applications (Figure 4), reinforces the conclusion that developmentally tuned JA pools essentially coordinate flower maturation and corolla opening. Most striking among the floral alterations documented in this study was that ir-*aoc*, *JMT/mje*, and the cross of *JMT/mje* with ir-*coi1* but not *COI1*-only silenced flowers failed to fully expand their corolla limbs during their lifetime. This could be due either to residual amounts of COI1 protein that are produced in the *COI1*-silenced RNA interference line selected for this study or to differences in the JA-Ile signaling thresholds required for organ-specific maturation outcomes. Variations in the COI1-dependent degradation of individual JAZ proteins have been reported previously (Shyu et al., 2012), which could potentially affect, in a tissue-specific manner, COI1-dependent maturation processes. Another explanation for the absence of alterations in the opening of ir-*coi1* flowers could be that this line can still perceive JA-Ile/COR signaling via an additional COI1-like protein that remains functional in this line.

Consistent with the conclusion that ir-*coi1* is sensitive to JA-Ile signaling flower opening is the observation that the defective limb opening of plants silenced for *COI1* and additionally impaired in JA-Ile biosynthesis (*JMT/mje* × ir-*coi1*) could be restored by the application of COR. Interestingly, defective limb opening could only be rescued for floral buds below a size of ~9 mm (Figure 5), suggesting that full limb opening depends on intact JA biosynthesis during early corolla elongation but that this does not require a functional COI1. With respect to timing, our results parallel previous reports concerning anther maturation, in which the authors demonstrated that the elongation of the filaments and the dehiscence of the anthers require JA biosynthesis before the bud opens (Sanders et al., 2000; Ito et al., 2007).

JA Homeostasis Underlies Floral Developmental Regulation

Oxylipin signatures differ significantly among floral organs (Hause et al., 2000), and JA biosynthesis has been shown to increase

after morphogenesis in female organs (Hause et al., 2000) and during flower maturation in anthers (Sanders et al., 2000; Ito et al., 2007). The regulation of JA biosynthesis is embedded into a partly understood transcriptional and signaling network that involves AGAMOUS plus ARF6 and ARF8 transcription factor activities (Nagpal et al., 2005; Ito et al., 2007). The analysis of tissue-specific JA dynamics presented in this study highlights the presence of a pronounced and transient increase in the size of the JA pools during maturation and demonstrates the existence of an independent regulation of the turnover of JA-Ile in the maturing corolla.

Redirecting JA toward MeJA formation in *JMT/mje* without altering the upstream flux allowed us to demonstrate that the peak of total corolla JA production is delayed for 2 d when the formation of active JA derivatives is disabled (Figures 2 and 3; Supplemental Figure 6), a pattern not observable in ir-*aoc* due to its completely disrupted JA synthesis. *Arabidopsis* knockout mutants for MYB21-5 and MYB24-5, two MYB305 homologs, show increased *cis*-jasmone levels in complete flowers due to an interruption of a negative feedback loop on JA biosynthesis mediated by these two transcription factors (Reeves et al., 2012). However, whereas the expression of MYB305 in dissected nectary tissues of *N. attenuata* ir-*aoc* and ir-*coi1* flowers was strongly impaired, that in corolla tissues was only delayed. This suggests that the JA- and COI1-dependent regulation of *MYB305* expression is strongly tissue specific in sympetalous flowers.

Decreases in total JAs, but not in JA-Ile pools, following COR treatment in wild-type and *JMT/mje* corollas are also consistent with the existence of negative feedback regulation of JA accumulation during corolla maturation. This feedback mechanism is regulated by JA-Ile/COI1 signaling and compensated by an additional COI1-mediated turnover regulation of JA-Ile levels. The differential developmental expression patterns of JA biosynthesis and signaling transcripts indicate that independent transcriptional set points shape JA homeostasis. Alternatively, it may be possible that this negative feedback mechanism is involved in the regulation of dynamic changes in the rate of floral organ growth, as the rate of corolla expansion is highly correlated with changes in JA pools.

The Duet of JA-Ile and COI1 Determines Traits for Pollinator Attraction

To maximize their outcrossing success, *N. attenuata* flowers attract night-active hawk moth pollinators (Euler and Baldwin, 1996) via BA emission and reward them with a floral nectar containing strongly varying concentrations of nicotine (which acts as a repellant) (Kessler et al., 2012). It has been shown previously that floral nectar secretion in *Brassica napus* can be increased by the application of various JAs, including JA-Ile and coronalon, another JA-Ile structural and functional homolog similar to COR (Radhika et al., 2010). These experiments assume that endogenous JA-Ile signaling modulates nectar secretion, but this assumption was not formally tested in these studies. We show that all silenced lines tested produce less or no (ir-*coi1*) nectar and possess immature nectaries, as indicated by the lack of orange-red coloration typical of mature wild-type nectaries. This clearly illustrates the essential character of JA-Ile/COI1 signaling for nectary maturation, the regulation of the synthesis of β-carotene pigments, and floral nectar secretion (Figure 6A).

In ornamental tobacco, the transcription factor MYB305 is primarily expressed in ripening nectaries and regulates nectary starch metabolism (Liu et al., 2009; Liu and Thornburg, 2012). MYB305 has been shown to regulate floral phenylpropanoid production, nectar secretion, and the accumulation of proteins such as NEC1 or Na-SWEET9, which together with its *Arabidopsis* homolog At-SWEET9 has recently been demonstrated to function as a sucrose efflux transporter essential for nectar secretion (Lin et al., 2014). The strongly reduced *MYB305* transcript levels in nectary tissues of ir-*aoc* (Figure 6) increased after COR application, and this treatment also partly restored the nectar secretion in ir-*aoc* flowers (Figure 6B). Consistent with the *MYB305*-dependent regulation of *NEC1*, we detected increased transcript levels of *NEC1* in COR-treated ir-*aoc* nectaries. However, the reduced expression of some genes coding for floral proteins could not be rescued by the COR treatment, as is the case of the *N. attenuata* homolog of an *Arabidopsis* nectary-specific β-*AMYLASE* (Shi et al., 2011). The JA dependency of *MYB305* expression in nectaries was further supported by tissue-specific transcript measurements in dissected floral tissues, showing that *MYB305* transcript levels were compromised in nectaries by COI1 silencing (Supplemental Figure 9).

Silencing the expression of the *MYB305* homolog *EOBII* in petunia (*Petunia hybrida*) results in floral corollas that fail to enter anthesis, whereas in *MYB305*-silenced *N. attenuata* plants, flowers abscised prematurely (Colquhoun et al., 2011). However, while the accumulation of *MYB305* transcripts was also delayed in dissected corolla tissues of ir-*coi1* and ir-*aoc* flowers, maximal levels at the onset of anthesis were similar to those of wild-type corollas at anthesis (Figure 3B). Interestingly, *Arabidopsis* mutants for *COI1* and the *MYB305* homologs *MYB21* and *MYB24* produce polypetalous flowers with delayed anther dehiscence that fail to open (Reeves et al., 2012), a phenotype that clearly distinguishes them from *N. attenuata* ir-*coi1* plants, which exhibit fully open sympetalous corollas. These phenotypic differences might be derived from a differential regulation of JAZ proteins modulating floral JA signaling or by different floral tissue-specific JA-Ile gradients, which in turn would differentially influence JAZ protein stability, as shown for JAZ8 in *Arabidopsis* (Shyu et al., 2012). Lines with defective limb opening failed to emit BA to the levels emitted from wild-type flowers (Figure 7A). Even though COR and MeJA treatments increase *CHAL1* transcript abundance, unaltered expression levels of this gene in ir-*coi1* flowers, which do not emit BA, point toward a JA-Ile-dependent regulation of BA formation/emission other than through limb opening or *CHAL1* expression, an hypothesis formulated previously by Ré et al. (2011).

Limb Opening Is Accompanied by a JA-Ile-Mediated Remodeling of Carbohydrate Metabolism

Monitoring floral opening during the first night of anthesis revealed no apparent time shift for full or partial limb expansion among the genotypes irrespective of the treatments (Figure 8A).

Anthesis is paralleled by a substantial increase in petal fresh mass, quantitatively caused by a water influx driven by a rapid increase in the cellular osmolarity of petal cells (Yap et al., 2008; Norikoshi et al., 2013). Interrupting or diverting JA biosynthesis resulted in lower limb fresh mass at the beginning and end of limb expansion (Figure 8B). The unaltered fresh mass of the ir-*coi1* limb suggests that residual amounts of the COI1 F-box protein may suffice for the regulation of limb fresh mass and complete expansion. Further rigorous investigations of this aspect of floral JA signaling will necessitate the use of knockout mutant lines for COI1. The substantial reduction in ABA levels in JA-deficient corollas suggests an important regulatory function of JA-Ile in the crosstalk between the JA and ABA signaling pathways. However, ABA complementation alone proved to be insufficient to rescue complete limb expansion (Supplemental Figure 11).

Several previous reports discussed the reprogramming of petal carbohydrate and energy metabolism that accompanies flower maturation and opening (Evans and Reid, 1988; Bieleski, 1993; Norikoshi et al., 2013). Gene Ontology (GO) enrichment analysis highlighted strong transcriptional modulations in floral energy metabolism of JA-deficient plants and indicates that JAs substantially regulate carbohydrate metabolism during floral maturation. In JA biosynthesis-deficient flowers, we found major alterations in limb carbohydrate and energy metabolism, whereby soluble sugars like fructose or combined glucose/hexoses and the intermediates of the TCA cycle were particularly affected (Figure 9). Interestingly, the level of malate, one of the major osmotica involved in the regulation of cellular turgor (Fernie and Martinoia, 2009; Sweetlove et al., 2010), was only slightly reduced in corollas of transgenic plants under control conditions and was unaltered after COR or MeJA treatments.

Little is known about macrometabolic remodeling occurring during corolla development. However, Müller et al. (2010) demonstrated that fundamental changes in floral primary metabolism can function in roles beyond osmotic regulation, and recent studies demonstrated signaling activity for sugars in plant development (Cho et al., 2006; Seo et al., 2011; Yang et al., 2013; Yu et al., 2013). We notably observed a correlation between the MeJA/COR-responsive increase in *CHAL1* transcripts and sugar levels in ir-*aoc* corollas, a pattern consistent with the previously reported sugar-dependent expression of *CHAL* in petunia (Tsukaya et al., 1991; Weiss et al., 1992; Moalem-Beno et al., 1997). This deregulation in energy metabolism might account for the defective limb opening, as indicated by the MeJA/COR-inducible restoration of primary metabolites and opening of ir-*aoc* and *JMT*/*mje* limbs. In this respect, this study demonstrates the regulatory function of the JA cascade over floral carbohydrate and energy metabolism, a process likely relevant to other plant species.

Altogether, our data provide robust evidence for JA-Ile's role as an essential regulator for synchronous organ maturation, floral volatile emission, and complete limb opening of sympetalous flowers at anthesis. Dissecting these complex interactions provides insights into floral JA homeostatic regulation and the largely unexplored interplay between JAs and floral sugar metabolism. Further investigations of the underlying regulatory network using multidisciplinary approaches such as the one presented here are likely to unravel additional molecular partners in JA signaling.

METHODS

Plant Material and Growth Conditions

Wild-type *Nicotiana attenuata* seeds from an inbred line in its 30th generation were used for all experiments. The original seeds were collected in 1988 from an isolated population at the DI ranch in southwestern Utah. Before germination on agar plates containing Gamborg B5 medium, all seeds were sterilized and incubated with diluted smoke (which is required for germination of dormant seeds) and 0.1 M gibberellic acid as described by Krügel et al. (2002). Plants silenced in different steps of the JA cascade were obtained from seeds of homozygote plants of previously described transgenic *N. attenuata* lines: ir-*aoc* (Kallenbach et al., 2012), ir-*coi1* (Paschold et al., 2007), and *JMT*/*mje* (Stitz et al., 2011b). Plants of all genotypes were grown with a day/night cycle of 16 h (26 to 28°C)/8 h (22 to 24°C) under supplemental light from Master Sun-T PIA Agro 400 or Master Sun-TPIA Plus 600-W sodium lamps (Philips).

Floral Morphology Analysis

Evening flowers fully open around 7:30 PM; therefore, all morphological measurements were conducted at that time. The starting point for recording corolla elongation and for the maturation timeline for flowers of all genotypes was the day when corolla tips started protruding from the sepals (1 DAP), which typically happened when buds had reached a length of ~8 mm. Subsequently, measurements of corolla lengths were conducted on a daily basis until all monitored buds had completed anthesis, the final stage for our examinations. These stages widely correspond to developmental stages 2 and 12 of ornamental tobacco (*Nicotiana tabacum*) and *Nicotiana tomentosiformis* flowers (Goldberg, 1988; Drews et al., 1992). At anthesis, the corolla limbs were straightened in order to allow for the measurement of the complete length of the corolla from its base below the nectary to the outer tip of the corolla limb.

Dimensions of single sepals, gynoecia, pistils, and filaments were recorded, after disruptive assessment of individual floral buds with constantly increasing corolla length (+0.5-mm steps), from 7 mm until anthesis using a digital caliper gauge with an accuracy of ±0.03 mm. The evening preceding the recording of the opening timeline, all open flowers were removed. The next day, individual floral buds at the right stage were labeled, and photographs were taken in 30-min intervals from 3 PM until completion of anthesis at 7:30 PM.

Relative Corolla Growth Calculation and Analysis of Organ-Specific Development

The duration of the corolla exponential phase is approximately 1 d longer in all JA biosynthesis/signaling transgenic plants tested (Supplemental Figure 3). Corolla, filament, pistil, gynoecium, and sepal sizes were recorded from independent flowers after dissection during the corolla exponential expansion phase of wild-type flowers (first 2 DAP, stages 1 to 3; range of wild-type corolla sizes, 8 to 25.3 mm). Data presented in Figure 2 were used to plot logarithmic growth graphs. To this end, ln-transformed 10 × corolla length (mm) values at each DAP presented in Figure 2A were used to conduct exponential regressions limited to the duration of the corolla exponential growth. Calculations were conducted in Excel 2010 independently for data sets corresponding to each genotype. The resulting equations were used to infer a relative developmental age expressed in DAP from the ln-transformed 10 × corolla length measurement presented in Figure 2. This developmental age was assigned to the different tissues dissected from a flower with a given corolla length. The

ln-transformed 10 × tissue sizes versus relative developmental ages are plotted in Supplemental Figure 3.

RGRs were calculated on a day basis using the corolla size data presented in Figure 2. Calculations were done according to Hill and Malmberg (1991), who described corolla RGR as the slope of ln(10 × corolla length) over time. The RGR is constant when absolute growth rate is exponential; for the duration of the exponential phase, we used the following equation: $RGR_{DAPi-j} = \ln(length_j/length_i)/(DAPi - DAPi)$.

Floral Restoration Treatments

For all experiments, plants were randomly assigned to treatment groups, and treatments were conducted when the apical bud cluster exposed first corollas outside of sepals. Treatments of wild-type and transgenic plants were conducted continuously for 3 weeks in the morning of every other day by dipping the complete apical bud cluster into treatment solutions. For restoration assays, plants were subjected to control (0.02% Tween and 0.1% ethanol), 500 μM JA-Ile, 100 μM MeJA (Sigma-Aldrich), 200 μM ABA (Sigma-Aldrich), or 1 μM COR (Sigma-Aldrich), each in an aqueous 0.02% Tween and 0.1% ethanol solution.

JA and ABA Analysis

Flowers used for all analyses were collected from the apical and three topmost branching inflorescences. Floral buds of all genotypes with the average length as measured for 1 to 5 DAP were harvested on the day after treatments. Tissues of flowers at anthesis were sampled in the early evening (7 PM) after the wild-type corolla limbs had completely unfolded. Immediately after the removal of floral buds, the sepals, gynoecium, and anthers were quickly removed and corollas were flash-frozen. Each of the three collected biological replicates was generated by pooling corolla tissues of >20 flowers of two individual plants. Approximately 50 mg of frozen tissues was homogenized to a fine powder by shaking with two steel beads (5 mm) in 2-mL reaction tubes using a Genogrinder (SPEX Certi Prep) at a frequency of 1200 strokes/min for 60 s. JA and ABA were extracted by shaking for 3 min with 1 mL of ethylacetate-containing internal standards for ABA [(+)-*cis*,*trans*-D_6-ABA], JA (9,10-D_2-dihydro-JA), JA-Ile (jasmonoyl-[$^{13}C_6$]isoleucine), and MeJA ([1,2,13-^{13}C]MeJA, synthesized by esterification of [1,2,13-$^{13}C_3$]JA with [^{13}C]methanol as described previously) (Zhang et al., 1997).

Samples were analyzed as described previously by Wang et al. (2007). Briefly, 10 μL of the resulting extracts was analyzed for JAs using a Varian 1200 L liquid chromatograph coupled to a triple quadrupole mass spectrometer (Varian) working with an electrospray ionization source. All JAs, with the exception of MeJA, were detected in the negative ionization mode. Tandem mass spectrometry transitions for selective detection were optimized as described by Stitz et al. (2011b). The JA internal standard response was used for the quantification of 12-OH-JA, 11-OH-JA, and OPDA, and concentrations were adjusted using previously calculated response factors. Peak response factors for OPDA (1.28) and hydroxy-JA (1.06) were applied as described previously (Stitz et al., 2011b). To avoid systematic errors inherent to transgenic line/treatment-specific differences in tissue fresh weight, concentrations were expressed per corolla after normalization by the fresh weight of a single dissected corolla for a given stage, genotype, and treatment.

For the statistical analysis of JA-Ile turnover (Supplemental Figure 8), Pearson correlation coefficients were calculated among the different JAs using biological replicate values at each DAP and for each genotype independently.

Gene Expression Analysis

Total RNA was extracted as described by Linke et al. (2002). RNA extracts were treated with DNase using the DNA-free kit from Applied Biosystems/Ambion. cDNA was synthesized from 2 μg of RNA using SuperScript II Reverse Transcriptase (Invitrogen) and a poly-T primer. Quantitative RT-PCR (qRT-PCR; Stratagene 500 Mx3005P) was conducted with 150 ng of cDNA using the core reagent kit (Eurogentec) and pairs of gene-specific primers (see below). qRT-PCR products were detected after reaction with SYBR Green (qPCR Core Kit for SYBR Green I; Eurogentec). Gene expression was calculated relative to the expression value of *N. attenuata ELONGATION FACTOR1-ALPHA* (*EF1*α). Primers used for qRT-PCR can be found in Supplemental Table 1.

Microarray Analysis

Floral buds of COR- and control-treated ir-*aoc* plants were harvested the morning before the flowers would open. Flowers were rapidly dissected, and nectary, pistil, and corolla tissues were separately flash-frozen in liquid nitrogen and used for RNA isolation. Total RNA was isolated with TRIZOL reagent, and copy RNA was labeled with the Quick Amp labeling kit (Agilent). Each sample was hybridized on Agilent single-color technology arrays (44K 60-mer oligonucleotide microarray designed for *N. attenuata* transcriptome analysis; Agilent). An Agilent microarray scanner (G2565BA) and Scan Control software were used to obtain the spot intensities. All microarray data with each probe name were deposited in the National Center for Biotechnology Information Gene Expression Omnibus (GEO) database (GSE52765). We confirm that all details are MIAME compliant. The resulting gene expression profiles were analyzed using GeneSpring GX software (Silicon Genetics). Raw intensities were normalized using the 75th percentile value and $\log_2$ and baseline transformed prior to statistical analysis. Probes were filtered based on their quality control metrics: correlation cutoff, 0.8; fold cutoff, 1.5; P value cutoff, 0.05.

Significantly overrepresented GO categories were identified using the BiNGO plugin for Cytoscape (Maere et al., 2005). A P value significance for each differentially regulated gene was calculated using a hypergeometric test with a Benjamini and Hochberg false discovery rate correction. $P < 0.05$ was used as the threshold for significantly enriched GO categories.

Floral Volatile Analysis

In the evening before the day of volatile collection, all open flowers were removed from the plants to prevent volatile trapping from flowers in their second night of anthesis. The next morning, individual flowers that were to open the night of the same day (5-DAP average length) were enclosed in food-quality plastic cups with a single hole on top. Two pieces of polydimethylsiloxane (PDMS; Roth) tubing of similar size were placed in each plastic cup at 3 PM, removed 21 h later, and stored at −20°C until further use. Two new pieces of PDMS tubing were placed (3 PM) into the containers to trap floral headspace volatiles during the second night of anthesis (21 h). Analysis of the absorbed volatile compounds was performed using a thermal desorption unit connected to a gas chromatograph-mass spectrometer (GCMS-QP2010) from Shimadzu equipped with a DB-5 column (Agilent). BA was identified by comparing its retention time and mass spectrum with those of a commercial BA standard (Sigma-Aldrich) analyzed with the same instrument and settings. Peak areas were integrated and normalized to the size of the PDMS tubing.

Nectar Secretion Assessment

N. attenuata flowers remain open for two consecutive nights, which necessitates ensuring that nectar is only collected from flowers of the same stage. For this reason, flowers that were to open for the first night of anthesis were labeled the morning before their first opening. Standing floral nectar volume was determined between 5 and 7 AM after the first night of anthesis by inserting a standardized 25-μL glass capillary into the corolla until it reached the tip of the ovary just above the nectary. To obtain complete nectar volumes, capillaries were held with one hand, the corolla tube with the other hand, and then, against the counterpressure of the

inserted capillary, corolla tubes were removed. This causes the nectar, due to the capillary effect, quantitatively to be sucked up the capillary, and nectar volume was then measured in millimeters in the capillary and converted into microliters as described (Kessler et al., 2008).

Carbohydrate and Primary Metabolite Analysis

Approximately 40 mg of flash-frozen limb tissues was homogenized to a fine powder by shaking with two steel beads (5 mm) in 2-mL reaction tubes using a Genogrinder (SPEX Certi Prep) at a frequency of 1200 strokes/min for 40 s. Metabolites were extracted by shaking for 1 min with 400 μL of 80% methanol and 20% ammonium acetate buffer (84 mM). One hundred microliters of each limb extract was dried and subsequently derivatized by methoximation/*N*-methyl-*N*-trimethylsilyltrifluoroacetamide, and afterward, 1 μL was analyzed by two-dimensional gas chromatography (6890N GC; Agilent Technologies) coupled to a Pegasus III time-of-flight mass spectrometer (LECO). LECO ChromaToF software version 4.34 was used to acquire and process the data (including automatic peak deconvolution). Processed peaks were reported at a signal-to-noise ratio of 10, since we previously estimated this value as the minimum value for accurate peak integration and identification of forward and reverse alignments (Gaquerel et al., 2009). Peak integration was first conducted using unique masses detected during automated deconvolution and then manually supervised for selectivity and sufficient intensity in order to improve the accuracy of peak area integration.

Metabolites reported in Figure 9 and Supplemental Figures 13 to 15 were identified by comparison of their 2D retention times, and mass spectra were identified by comparison with those of authentic standards analyzed under the same conditions. Metabolites of interest (phenylalanine, quinic acid, and fumarate) for which no standard was available were annotated, after manually supervised automated mass spectral matching, with thresholds set to match factor >650 (maximum match, 1000) and retention time deviation <10%, based on the mass spectral and retention time collection data available at the Golm Metabolome Database (http://gmd.mpimp-golm.mpg.de/search.aspx). Results were calculated for 1 g of dry limb tissue. Dry weights were determined following drying to a constant weight in a forced draft oven at 80°C.

Statistical Analysis

Most statistical analyses were performed with StatView (Abacus Concepts; http://www.statview.com), and the general level of significance applied was $\alpha = 0.05$. JA pools were calculated for corollas of each DAP by summing, for each treatment, the average ($n = 3$) OPDA, JA, MeJA, hydroxy-JA, JA-Glc, and JA-Ile levels of individual corolla samples. JA pools were then presented as bar charts and analyzed by Student's *t* test.

All other statistical analyses were conducted with SPSS 17.0 (IBM). One- and two-factorial ANOVAs were followed by Bonferroni/Tukey posthoc tests. When necessary, data were $\log_2$ transformed (BA) or square root transformed (transcript abundance of *MYB305* and *NEC1* in nectary tissue). Bonferroni P value corrections were used to correct for nonparametric multiple comparisons.

Accession Numbers

The GenBank accession numbers for the most relevant genes discussed in this article are as follows: *N. attenuata AOC* (EF467332), *AOS* (AJ295274), *OPR3* (EF467331), *MJE* (EU196055), *Arabidopsis JMT* (DI053904), *N. attenuata TD* (AY928105), *COI1* (EF025087), *JAZd* (JQ172762), *MYB305* (GT184412), and *CHAL1* (EU503226). Results of the microarray analysis (microarray platform; GEO accession number GPL13527) were deposited in the National Center for Biotechnology Information GEO database (GSE52765).

Supplemental Data

The following materials are available in the online version of this article.

Supplemental Figure 1. *COI1* Transcript Levels Are Silenced to Similar Levels in All Floral Tissues of ir-*coi1* Plants.

Supplemental Figure 2. The Growth Rate of Different Flower Organs Is Altered in JA Biosynthesis/Perception-Deficient Transgenic Lines during Rapid Corolla Elongation.

Supplemental Figure 3. Relative Growth Rate Calculations Indicate Phase-Specific Effects of JA Signaling Deficiency on Corolla Growth.

Supplemental Figure 4. Delayed Maturation of ir-*aoc*, *JMT/mje*, and ir-*coi1* Cannot Be Recovered by MeJA or Coronatine (COR) Treatment.

Supplemental Figure 5. Crosses between Wild-Type and ir-*coi1* and *JMT/mje* Plants Exhibit Corolla Phenotypes of Their Transgenic Parents.

Supplemental Figure 6. COR Application Reveals a Negative Feedback Effect of JA-Ile Signaling on Developmentally Regulated JA Pools of Corollas.

Supplemental Figure 7. Reduced *TD* Transcript Levels in JAs but Not in COI1-Deficient Corollas Are Partly Rescued by MeJA/COR Application.

Supplemental Figure 8. Silencing *COI1* Expression Remodels Developmentally Regulated Effects on JA-Ile Accumulation.

Supplemental Figure 9. Floral Expression of *MYB305* Primarily Expressed in Nectary Tissues Is Impaired in COI1-Deficient Nectaries.

Supplemental Figure 10. Developmentally Regulated Abscisic Acid (ABA) Accumulation during Corolla Expansion Involves COR/JA-Ile Signaling.

Supplemental Figure 11. ABA Treatment Does Not Restore Corolla Limb Opening in JA-Deficient Flowers.

Supplemental Figure 12. Coronatine Application on ir-*aoc* Flowers Activates Transcriptomic Changes in Flower Signaling, Metabolic, and Developmental Processes.

Supplemental Figure 13. BINGO Analysis of Biological Process Overrepresentation.

Supplemental Figure 14. Accumulation of Carbohydrates and Intermediates of Energy Metabolism in Limbs at Anthesis Is Altered in Lines with Alterations in the JA Signaling Cascade.

Supplemental Figure 15. Developmental Changes in Carbohydrate Composition and Accumulation of Intermediates of the TCA Cycle during Anthesis Are Regulated via JA Signaling.

Supplemental Figure 16. Limb Accumulation of Some Amino Acids and Other Metabolites Is Compromised by JA Deficiency and Can Be Rescued by MeJA or COR Applications.

Supplemental Table 1. Sequences of Gene-Specific Primers Used for qRT-PCR.

Supplemental Data Set 1. List of All Genes Regulated in *N. attenuata* Floral Tissues after Coronatine Treatment.

ACKNOWLEDGMENTS

We thank Matthias Schöttner and Mario Kallenbach for technical help with metabolic analyses, Klaus Gase for help with the microarray analysis, Variluska Fragoso and Felipe Yon for help in the greenhouse,

and Mariana Stanton, Gustavo Bonaventure, and Youngjoo Oh for helpful discussions. This work was supported by the Max Planck Society. E.G.'s research was funded by Advanced Grant 293926 of the European Research Council to I.T.B.

AUTHOR CONTRIBUTIONS

M.S. designed and performed the research, evaluated the data, and wrote the article. E.G. designed the research, evaluated data, and wrote the article. M.H. performed research. I.T.B. wrote the article.

Received June 3, 2014; revised September 17, 2014; accepted October 1, 2014; published October 17, 2014.

REFERENCES

Abe, I., Takahashi, Y., Morita, H., and Noguchi, H. (2001). Benzalacetone synthase. A novel polyketide synthase that plays a crucial role in the biosynthesis of phenylbutanones in *Rheum palmatum*. Eur. J. Biochem. **268:** 3354–3359.

Babst, B.A., Ferrieri, R.A., Gray, D.W., Lerdau, M., Schlyer, D.J., Schueller, M., Thorpe, M.R., and Orians, C.M. (2005). Jasmonic acid induces rapid changes in carbon transport and partitioning in Populus. New Phytol. **167:** 63–72.

Baldwin, I.T., Preston, C., Euler, M., and Gorham, D. (1997). Patterns and consequences of benzyl acetone floral emissions from *Nicotiana attenuata* plants. J. Chem. Ecol. **23:** 2327–2343.

Bieleski, R.L. (1993). Fructan hydrolysis drives petal expansion in the ephemeral daylily flower. Plant Physiol. **103:** 213–219.

Blechert, S., Brodschelm, W., Hölder, S., Kammerer, L., Kutchan, T.M., Mueller, M.J., Xia, Z.Q., and Zenk, M.H. (1995). The octadecanoic pathway: Signal molecules for the regulation of secondary pathways. Proc. Natl. Acad. Sci. USA **92:** 4099–4105.

Brioudes, F., Joly, C., Szécsi, J., Varaud, E., Leroux, J., Bellvert, F., Bertrand, C., and Bendahmane, M. (2009). Jasmonate controls late development stages of petal growth in *Arabidopsis thaliana*. Plant J. **60:** 1070–1080.

Campbell, S.A., Thaler, J.S., and Kessler, A. (2013). Plant chemistry underlies herbivore-mediated inbreeding depression in nature. Ecol. Lett. **16:** 252–260.

Cecchetti, V., Altamura, M.M., Brunetti, P., Petrocelli, V., Falasca, G., Ljung, K., Costantino, P., and Cardarelli, M. (2013). Auxin controls Arabidopsis anther dehiscence by regulating endothecium lignification and jasmonic acid biosynthesis. Plant J. **74:** 411–422.

Chandler, J.W. (2010). The hormonal regulation of flower development. J. Plant Growth Regul. **30:** 242–254.

Cheng, Y., Dai, X., and Zhao, Y. (2006). Auxin biosynthesis by the YUCCA flavin monooxygenases controls the formation of floral organs and vascular tissues in Arabidopsis. Genes Dev. **20:** 1790–1799.

Cheng, Z., Sun, L., Qi, T., Zhang, B., Peng, W., Liu, Y., and Xie, D. (2011). The bHLH transcription factor MYC3 interacts with the jasmonate ZIM-domain proteins to mediate jasmonate response in Arabidopsis. Mol. Plant **4:** 279–288.

Chini, A., Fonseca, S., Chico, J.M., Fernández-Calvo, P., and Solano, R. (2009). The ZIM domain mediates homo- and heteromeric interactions between Arabidopsis JAZ proteins. Plant J. **59:** 77–87.

Chini, A., Fonseca, S., Fernández, G., Adie, B., Chico, J.M., Lorenzo, O., García-Casado, G., López-Vidriero, I., Lozano, F.M., Ponce, M.R., Micol, J.L., and Solano, R. (2007). The JAZ family of repressors is the missing link in jasmonate signalling. Nature **448:** 666–671.

Cho, Y.-H., Yoo, S.-D., and Sheen, J. (2006). Regulatory functions of nuclear hexokinase1 complex in glucose signaling. Cell **127:** 579–589.

Colquhoun, T.A., Schwieterman, M.L., Wedde, A.E., Schimmel, B.C., Marciniak, D.M., Verdonk, J.C., Kim, J.Y., Oh, Y., Gális, I., Baldwin, I.T., and Clark, D.G. (2011). EOBII controls flower opening by functioning as a general transcriptomic switch. Plant Physiol. **156:** 974–984.

Creelman, R.A., and Mullet, J.E. (1995). Jasmonic acid distribution and action in plants: regulation during development and response to biotic and abiotic stress. Proc. Natl. Acad. Sci. USA **92:** 4114–4119.

Delph, L., and Lively, C. (1989). The evolution of floral color change: Pollinator attraction versus physiological constraints in *Fuchsia excorticata*. Evolution **43:** 1252–1262.

Drews, G.N., Beals, T.P., Bui, A.Q., and Goldberg, R.B. (1992). Regional and cell-specific gene expression patterns during petal development. Plant Cell **4:** 1383–1404.

Dubos, C., Stracke, R., Grotewold, E., Weisshaar, B., Martin, C., and Lepiniec, L. (2010). MYB transcription factors in Arabidopsis. Trends Plant Sci. **15:** 573–581.

Dudareva, N., Murfitt, L.M., Mann, C.J., Gorenstein, N., Kolosova, N., Kish, C.M., Bonham, C., and Wood, K. (2000). Developmental regulation of methyl benzoate biosynthesis and emission in snapdragon flowers. Plant Cell **12:** 949–961.

Esau, K. (1977). Anatomy of Seed Plants, 2nd ed. (New York: John Wiley & Sons).

Euler, M., and Baldwin, I.T. (1996). The chemistry of defense and apparency in the corollas of *Nicotiana attenuata*. Oecologia **107:** 102–112.

Evans, R., and Reid, M. (1988). Changes in carbohydrates and osmotic potential during rhythmic expansion of rose petals. J. Am. Soc. Hortic. **113:** 884–888.

Fernie, A.R., and Martinoia, E. (2009). Malate. Jack of all trades or master of a few? Phytochemistry **70:** 828–832.

Feys, B., Benedetti, C.E., Penfold, C.N., and Turner, J.G. (1994). *Arabidopsis* mutants selected for resistance to the phytotoxin coronatine are male sterile, insensitive to methyl jasmonate, and resistant to a bacterial pathogen. Plant Cell **6:** 751–759.

Fonseca, S., Chini, A., Hamberg, M., Adie, B., Porzel, A., Kramell, R., Miersch, O., Wasternack, C., and Solano, R. (2009). (+)-7-iso-Jasmonoyl-L-isoleucine is the endogenous bioactive jasmonate. Nat. Chem. Biol. **5:** 344–350.

Gaquerel, E., Weinhold, A., and Baldwin, I.T. (2009). Molecular interactions between the specialist herbivore *Manduca sexta* (Lepidoptera, Sphigidae) and its natural host *Nicotiana attenuata*. VIII. An unbiased GCxGC-ToFMS analysis of the plant's elicited volatile emissions. Plant Physiol. **149:** 1408–1423.

Gfeller, A., Dubugnon, L., Liechti, R., and Farmer, E.E. (2010). Jasmonate biochemical pathway. Sci. Signal. **3:** cm3.

Goetz, S., Hellwege, A., Stenzel, I., Kutter, C., Hauptmann, V., Forner, S., McCaig, B., Hause, G., Miersch, O., Wasternack, C., and Hause, B. (2012). Role of cis-12-oxo-phytodienoic acid in tomato embryo development. Plant Physiol. **158:** 1715–1727.

Goldberg, R.B. (1988). Plants: Novel developmental processes. Science **240:** 1460–1467.

Greulichi, F., Yoshihara, T., and Ichihara, A. (1995). Coronatine, a bacterial phytotoxin, acts as a stereospecific analog of jasmonate type signals in tomato cells and potato tissues. J. Plant Physiol. **147:** 359–366.

Hause, B., Stenzel, I., Miersch, O., Maucher, H., Kramell, R., Ziegler, J., and Wasternack, C. (2000). Tissue-specific oxylipin

signature of tomato flowers: Allene oxide cyclase is highly expressed in distinct flower organs and vascular bundles. Plant J. **24:** 113–126.

Hill, J.P., and Malmberg, R.L. (1991). Rates of corolla growth in tobacco determined with the plastochron index. Planta **185:** 472–478.

Hoballah, M.E., Gübitz, T., Stuurman, J., Broger, L., Barone, M., Mandel, T., Dell'Olivo, A., Arnold, M., and Kuhlemeier, C. (2007). Single gene-mediated shift in pollinator attraction in *Petunia*. Plant Cell **19:** 779–790.

Hou, X., Hu, W.-W., Shen, L., Lee, L.Y.C., Tao, Z., Han, J.-H., and Yu, H. (2008). Global identification of DELLA target genes during Arabidopsis flower development. Plant Physiol. **147:** 1126–1142.

Huang, S., Cerny, R.E., Qi, Y., Bhat, D., Aydt, C.M., Hanson, D.D., Malloy, K.P., and Ness, L.A. (2003). Transgenic studies on the involvement of cytokinin and gibberellin in male development. Plant Physiol. **131:** 1270–1282.

Ichimura, K., Kohata, K., Yamaguchi, Y., Douzono, M., Ikeda, H., and Koketsu, M. (2000). Identification of L-inositol and scyllitol and their distribution in various organs in chrysanthemum. Biosci. Biotechnol. Biochem. **64:** 865–868.

Ishiguro, S., Kawai-Oda, A., Ueda, J., Nishida, I., and Okada, K. (2001). The DEFECTIVE IN ANTHER DEHISCIENCE gene encodes a novel phospholipase A1 catalyzing the initial step of jasmonic acid biosynthesis, which synchronizes pollen maturation, anther dehiscence, and flower opening in *Arabidopsis*. Plant Cell **13:** 2191–2209.

Ito, T., Ng, K.-H., Lim, T.-S., Yu, H., and Meyerowitz, E.M. (2007). The homeotic protein AGAMOUS controls late stamen development by regulating a jasmonate biosynthetic gene in *Arabidopsis*. Plant Cell **19:** 3516–3529.

Jackson, D., Roberts, K., and Martin, C. (1992). Temporal and spatial control of expression of anthocyanin biosynthetic genes in developing flowers of *Antirrhinum majus*. Plant J. **2:** 425–434.

Kallenbach, M., Alagna, F., Baldwin, I.T., and Bonaventure, G. (2010). *Nicotiana attenuata* SIPK, WIPK, NPR1, and fatty acid-amino acid conjugates participate in the induction of jasmonic acid biosynthesis by affecting early enzymatic steps in the pathway. Plant Physiol. **152:** 96–106.

Kallenbach, M., Bonaventure, G., Gilardoni, P.A., Wissgott, A., and Baldwin, I.T. (2012). Empoasca leafhoppers attack wild tobacco plants in a jasmonate-dependent manner and identify jasmonate mutants in natural populations. Proc. Natl. Acad. Sci. USA **109:** E1548–E1557.

Kang, J.-H., Wang, L., Giri, A., and Baldwin, I.T. (2006). Silencing threonine deaminase and JAR4 in *Nicotiana attenuata* impairs jasmonic acid-isoleucine-mediated defenses against *Manduca sexta*. Plant Cell **18:** 3303–3320.

Katsir, L., Chung, H.S., Koo, A.J.K., and Howe, G.A. (2008). Jasmonate signaling: A conserved mechanism of hormone sensing. Curr. Opin. Plant Biol. **11:** 428–435.

Kessler, D., Bhattacharya, S., Diezel, C., Rothe, E., Gase, K., Schöttner, M., and Baldwin, I.T. (2012). Unpredictability of nectar nicotine promotes outcrossing by hummingbirds in *Nicotiana attenuata*. Plant J. **71:** 529–538.

Kessler, D., Diezel, C., and Baldwin, I.T. (2010). Changing pollinators as a means of escaping herbivores. Curr. Biol. **20:** 237–242.

Kessler, D., Gase, K., and Baldwin, I.T. (2008). Field experiments with transformed plants reveal the sense of floral scents. Science **321:** 1200–1202.

Koning, R.E. (1986). The role of ethylene in corolla unfolding in *Ipomoea nil* (Convolvulaceae). Am. J. Bot. **73:** 152–155.

Koo, A.J.K., Cooke, T.F., and Howe, G.A. (2011). Cytochrome P450 CYP94B3 mediates catabolism and inactivation of the plant hormone jasmonoyl-L-isoleucine. Proc. Natl. Acad. Sci. USA **108:** 9298–9303.

Koornneef, M., and van der Veen, J.H. (1980). Induction and analysis of gibberellin sensitive mutants in *Arabidopsis thaliana* (L.) Heynh. Theor. Appl. Genet. **58:** 257–263.

Krügel, T., Lim, M., Gase, K., Halitschke, R., and Baldwin, I.T. (2002). Agrobacterium-mediated transformation of *Nicotiana attenuata*, a model ecological expression system. Chemoecology **12:** 177–183.

Krumm, T., Bandemer, K., and Boland, W. (1995). Induction of volatile biosynthesis in the lima bean (*Phaseolus lunatus*) by leucine- and isoleucine conjugates of 1-oxo- and 1-hydroxyindan-4-carboxylic acid: Evidence for amino acid conjugates of jasmonic acid as intermediates in the octadecanoid signalling pathway. FEBS Lett. **377:** 523–529.

Kuipef, D., Ribot, S., Van Reenen, H.S., and Marissenb, N. (1995). The effect of sucrose on the flower bud opening of "Madelon" cut roses. Sci. Hortic. (Amsterdam) **60:** 325–336.

Li, L., Li, C., and Howe, G.A. (2001). Genetic analysis of wound signaling in tomato: Evidence for a dual role of jasmonic acid in defense and female fertility. Plant Physiol. **127:** 1414–1417.

Li, L., Zhao, Y., McCaig, B.C., Wingerd, B.A., Wang, J., Whalon, M.E., Pichersky, E., and Howe, G.A. (2004). The tomato homolog of CORONATINE-INSENSITIVE1 is required for the maternal control of seed maturation, jasmonate-signaled defense responses, and glandular trichome development. Plant Cell **16:** 126–143.

Lin, I.W., et al. (2014). Nectar secretion requires sucrose phosphate synthases and the sugar transporter SWEET9. Nature, in press

Linke, C., Conrath, U., Jeblick, W., Betsche, T., Mahn, A., and Du, K. (2002). Inhibition of the plastidic ATP/ADP transporter protein primes potato tubers for augmented elicitation of defense responses and enhances their resistance against *Erwinia carotovora*. Plant Physiol. **129:** 1607–1615.

Liu, G., and Thornburg, R.W. (2012). Knockdown of MYB305 disrupts nectary starch metabolism and floral nectar production. Plant J. **70:** 377–388.

Liu, G., Ren, G., Guirgis, A., and Thornburg, R.W. (2009). The MYB305 transcription factor regulates expression of nectarin genes in the ornamental tobacco floral nectary. Plant Cell **21:** 2672–2687.

Maere, S., Heymans, K., and Kuiper, M. (2005). BiNGO: A Cytoscape plugin to assess overrepresentation of Gene Ontology categories in biological networks. Bioinformatics **21:** 3448–3449.

Martinoia, E., Maeshima, M., and Neuhaus, H.E. (2007). Vacuolar transporters and their essential role in plant metabolism. J. Exp. Bot. **58:** 83–102.

Miernyk, J.A., and Randall, D.D. (1987). Some kinetic and regulatory properties of the pea mitochondrial pyruvate dehydrogenase complex. Plant Physiol. **83:** 306–310.

Miersch, O., Weichert, H., Stenzel, I., Hause, B., Maucher, H., Feussner, I., and Wasternack, C. (2004). Constitutive overexpression of allene oxide cyclase in tomato (*Lycopersicon esculentum* cv. Lukullus) elevates levels of some jasmonates and octadecanoids in flower organs but not in leaves. Phytochemistry **65:** 847–856.

Moalem-Beno, D., Tamari, G., Leitner-Dagan, Y., Borochov, A., and Weiss, D. (1997). Sugar-dependent gibberellin-induced chalcone synthase gene expression in petunia corollas. Plant Physiol. **113:** 419–424.

Müller, G.L., Drincovich, M.F., Andreo, C.S., and Lara, M.V. (2010). Role of photosynthesis and analysis of key enzymes involved in primary metabolism throughout the lifespan of the tobacco flower. J. Exp. Bot. **61:** 3675–3688.

Nagpal, P., Ellis, C.M., Weber, H., Ploense, S.E., Barkawi, L.S., Guilfoyle, T.J., Hagen, G., Alonso, J.M., Cohen, J.D., Farmer, E.E.,

Ecker, J.R., and Reed, J.W. (2005). Auxin response factors ARF6 and ARF8 promote jasmonic acid production and flower maturation. Development **132:** 4107–4118.

Nilsson, L. (1988). The evolution of flowers with deep corolla tubes. Nature **334:** 147–149.

Norikoshi, R., Imanishi, H., and Ichimura, K. (2013). Changes in cell number, osmotic potential and concentrations of carbohydrates and inorganic ions in *Tweedia caerulea* during flower opening. J. Jpn. Soc. Hortic. Sci. **82:** 51–56.

Oh, Y., Baldwin, I.T., and Galis, I. (2013). A jasmonate ZIM-domain protein NaJAZd regulates floral jasmonic acid levels and counteracts flower abscission in *Nicotiana attenuata* plants. PLoS ONE **8:** e57868.

Oliver, S.N., Dennis, E.S., and Dolferus, R. (2007). ABA regulates apoplastic sugar transport and is a potential signal for cold-induced pollen sterility in rice. Plant Cell Physiol. **48:** 1319–1330.

Østergaard, L. (2009). Don't 'leaf' now. The making of a fruit. Curr. Opin. Plant Biol. **12:** 36–41.

Park, S.-W., et al. (2013). Cyclophilin 20-3 relays a 12-oxo-phytodienoic acid signal during stress responsive regulation of cellular redox homeostasis. Proc. Natl. Acad. Sci. USA **110:** 9559–9564.

Paschold, A., Bonaventure, G., Kant, M.R., and Baldwin, I.T. (2008). Jasmonate perception regulates jasmonate biosynthesis and JA-Ile metabolism: The case of COI1 in *Nicotiana attenuata*. Plant Cell Physiol. **49:** 1165–1175.

Paschold, A., Halitschke, R., and Baldwin, I.T. (2007). Co(i)-ordinating defenses: NaCOI1 mediates herbivore- induced resistance in *Nicotiana attenuata* and reveals the role of herbivore movement in avoiding defenses. Plant J. **51:** 79–91.

Popova, T.N., and Pinheiro de Carvalho, M.A. (1998). Citrate and isocitrate in plant metabolism. Biochim. Biophys. Acta **1364:** 307–325.

Qi, T., Song, S., Ren, Q., Wu, D., Huang, H., Chen, Y., Fan, M., Peng, W., Ren, C., and Xie, D. (2011). The jasmonate-ZIM-domain proteins interact with the WD-Repeat/bHLH/MYB complexes to regulate jasmonate-mediated anthocyanin accumulation and trichome initiation in *Arabidopsis thaliana*. Plant Cell **23:** 1795–1814.

Radhika, V., Kost, C., Boland, W., and Heil, M. (2010). The role of jasmonates in floral nectar secretion. PLoS ONE **5:** e9265.

Raven, P.H., Evert, R.F., and Eichhorn, S.E. (1986). Biology of Plants, 18th ed. (New York: Worth Publishers).

Ré, D.A., Dezar, C.A., Chan, R.L., Baldwin, I.T., and Bonaventure, G. (2011). *Nicotiana attenuata* NaHD20 plays a role in leaf ABA accumulation during water stress, benzylacetone emission from flowers, and the timing of bolting and flower transitions. J. Exp. Bot. **62:** 155–166.

Reeves, P.H., et al. (2012). A regulatory network for coordinated flower maturation. PLoS Genet. **8:** e1002506.

Sanders, P.M., Lee, P.Y., Biesgen, C., Boone, J.D., Beals, T.P., Weiler, E.W., and Goldberg, R.B. (2000). The *Arabidopsis* DELAYED DEHISCENCE1 gene encodes an enzyme in the jasmonic acid synthesis pathway. Plant Cell **12:** 1041–1061.

Schaller, A., and Stintzi, A. (2009). Enzymes in jasmonate biosynthesis: Structure, function, regulation. Phytochemistry **70:** 1532–1538.

Schaller, F. (2001). Enzymes of the biosynthesis of octadecanoid-derived signalling molecules. J. Exp. Bot. **52:** 11–23.

Seo, P.J., Ryu, J., Kang, S.K., and Park, C.-M. (2011). Modulation of sugar metabolism by an INDETERMINATE DOMAIN transcription factor contributes to photoperiodic flowering in Arabidopsis. Plant J. **65:** 418–429.

Shang, Y., Venail, J., Mackay, S., Bailey, P.C., Schwinn, K.E., Jameson, P.E., Martin, C.R., and Davies, K.M. (2011). The molecular basis for venation patterning of pigmentation and its effect on pollinator attraction in flowers of Antirrhinum. New Phytol. **189:** 602–615.

Shi, J.X., Malitsky, S., De Oliveira, S., Branigan, C., Franke, R.B., Schreiber, L., and Aharoni, A. (2011). SHINE transcription factors act redundantly to pattern the archetypal surface of Arabidopsis flower organs. PLoS Genet. **7:** e1001388.

Shyu, C., Figueroa, P., Depew, C.L., Cooke, T.F., Sheard, L.B., Moreno, J.E., Katsir, L., Zheng, N., Browse, J., and Howe, G.A. (2012). JAZ8 lacks a canonical degron and has an EAR motif that mediates transcriptional repression of jasmonate responses in *Arabidopsis*. Plant Cell **24:** 536–550.

Smyth, D.R., Bowman, J.L., and Meyerowitz, E.M. (1990). Early flower development in *Arabidopsis*. Plant Cell **2:** 755–767.

Song, S., Qi, T., Huang, H., Ren, Q., Wu, D., Chang, C., Peng, W., Liu, Y., Peng, J., and Xie, D. (2011). The jasmonate-ZIM domain proteins interact with the R2R3-MYB transcription factors MYB21 and MYB24 to affect jasmonate-regulated stamen development in *Arabidopsis*. Plant Cell **23:** 1000–1013.

Stanton, M.L., Snow, A.A., and Handel, S.N. (1986). Floral evolution: Attractiveness to pollinators increases male fitness. Science **232:** 1625–1627.

Staswick, P.E., and Tiryaki, I. (2004). The oxylipin signal jasmonic acid is activated by an enzyme that conjugates it to isoleucine in *Arabidopsis*. Plant Cell **16:** 2117–2127.

Stitz, M., Baldwin, I.T., and Gaquerel, E. (2011a). Diverting the flux of the JA pathway in *Nicotiana attenuata* compromises the plant's defense metabolism and fitness in nature and glasshouse. PLoS ONE **6:** e25925.

Stitz, M., Gase, K., Baldwin, I.T., and Gaquerel, E. (2011b). Ectopic expression of AtJMT in *Nicotiana attenuata*: Creating a metabolic sink has tissue-specific consequences for the jasmonate metabolic network and silences downstream gene expression. Plant Physiol. **157:** 341–354.

Sweetlove, L.J., Beard, K.F.M., Nunes-Nesi, A., Fernie, A.R., and Ratcliffe, R.G. (2010). Not just a circle: Flux modes in the plant TCA cycle. Trends Plant Sci. **15:** 462–470.

Szécsi, J., Joly, C., Bordji, K., Varaud, E., Cock, J.M., Dumas, C., and Bendahmane, M. (2006). BIGPETALp, a bHLH transcription factor is involved in the control of Arabidopsis petal size. EMBO J. **25:** 3912–3920.

Tejeda-Sartorius, M., Martínez de la Vega, O., and Délano-Frier, J.P. (2008). Jasmonic acid influences mycorrhizal colonization in tomato plants by modifying the expression of genes involved in carbohydrate partitioning. Physiol. Plant. **133:** 339–353.

Thines, B., Katsir, L., Melotto, M., Niu, Y., Mandaokar, A., Liu, G., Nomura, K., He, S.Y., Howe, G.A., and Browse, J. (2007). JAZ repressor proteins are targets of the SCF(COI1) complex during jasmonate signalling. Nature **448:** 661–665.

Tsukaya, H., Ohshima, T., Naito, S., Chino, M., and Komeda, Y. (1991). Sugar-dependent expression of the CHS-A gene for chalcone synthase from petunia in transgenic Arabidopsis. Plant Physiol. **97:** 1414–1421.

Varaud, E., Brioudes, F., Szécsi, J., Leroux, J., Brown, S., Perrot-Rechenmann, C., and Bendahmane, M. (2011). AUXIN RESPONSE FACTOR8 regulates *Arabidopsis* petal growth by interacting with the bHLH transcription factor BIGPETALp. Plant Cell **23:** 973–983.

Vergauwen, R., Van den Ende, W., and Van Laere, A. (2000). The role of fructan in flowering of *Campanula rapunculoides*. J. Exp. Bot. **51:** 1261–1266.

Vick, B.A., and Zimmerman, D.C. (1983). The biosynthesis of jasmonic acid: A physiological role for plant lipoxygenase. Biochem. Biophys. Res. Commun. **111:** 470–477.

Wahl, V., Ponnu, J., Schlereth, A., Arrivault, S., Langenecker, T., Franke, A., Feil, R., Lunn, J.E., Stitt, M., and Schmid, M. (2013). Regulation of flowering by trehalose-6-phosphate signaling in *Arabidopsis thaliana*. Science **339:** 704–707.

Wang, L., Halitschke, R., Kang, J.-H., Berg, A., Harnisch, F., and Baldwin, I.T. (2007). Independently silencing two JAR family members impairs levels of trypsin proteinase inhibitors but not nicotine. Planta **226:** 159–167.

Wang, Z., Dai, L., Jiang, Z., Peng, W., Zhang, L., Wang, G., and Xie, D. (2005). GmCOI1, a soybean F-box protein gene, shows ability to mediate jasmonate-regulated plant defense and fertility in Arabidopsis. Mol. Plant Microbe Interact. **18:** 1285–1295.

Wasternack, C. (2007). Jasmonates: An update on biosynthesis, signal transduction and action in plant stress response, growth and development. Ann. Bot. (Lond.) **100:** 681–697.

Wasternack, C., Forner, S., Strnad, M., and Hause, B. (2013). Jasmonates in flower and seed development. Biochimie **95:** 79–85.

Weiss, D., van Blokland, R., Kooter, J.M., Mol, J.N., and van Tunen, A.J. (1992). Gibberellic acid regulates chalcone synthase gene transcription in the corolla of *Petunia hybrida*. Plant Physiol. **98:** 191–197.

Weiss, D., Van Der Luit, A., Knegt, E., Vermeer, E., Mol, J., and Kooter, J.M. (1995). Identification of endogenous gibberellins in petunia flowers (induction of anthocyanin biosynthetic gene expression and the antagonistic effect of abscisic acid). Plant Physiol. **107:** 695–702.

Xie, D.X., Feys, B.F., James, S., Nieto-Rostro, M., and Turner, J.G. (1998). COI1: An Arabidopsis gene required for jasmonate-regulated defense and fertility. Science **280:** 1091–1094.

Yan, J., Zhang, C., Gu, M., Bai, Z., Zhang, W., Qi, T., Cheng, Z., Peng, W., Luo, H., Nan, F., Wang, Z., and Xie, D. (2009). The *Arabidopsis* CORONATINE INSENSITIVE1 protein is a jasmonate receptor. Plant Cell **21:** 2220–2236.

Yan, Y., Stolz, S., Chételat, A., Reymond, P., Pagni, M., Dubugnon, L., and Farmer, E.E. (2007). A downstream mediator in the growth repression limb of the jasmonate pathway. Plant Cell **19:** 2470–2483.

Yang, L., Xu, M., Koo, Y., He, J., and Poethig, R.S. (2013). Sugar promotes vegetative phase change in *Arabidopsis thaliana* by repressing the expression of MIR156A and MIR156C. eLife **2:** e00260.

Yap, Y.-M., Loh, C.-S., and Ong, B.-L. (2008). Regulation of flower development in *Dendrobium crumenatum* by changes in carbohydrate contents, water status and cell wall metabolism. Sci. Hortic. (Amsterdam) **119:** 59–66.

Ye, M., Luo, S.M., Xie, J.F., Li, Y.F., Xu, T., Liu, Y., Song, Y.Y., Zhu-Salzman, K., and Zeng, R.S. (2012). Silencing COI1 in rice increases susceptibility to chewing insects and impairs inducible defense. PLoS ONE **7:** e36214.

Yu, S., Cao, L., Zhou, C.-M., Zhang, T.-Q., Lian, H., Sun, Y., Wu, J., Huang, J., Wang, G., and Wang, J.-W. (2013). Sugar is an endogenous cue for juvenile-to-adult phase transition in plants. eLife **2:** e00269.

Zhang, Z., Krumm, T., and Baldwin, I. (1997). Structural requirements of jasmonates and mimics for nicotine induction in *Nicotiana sylvestris*. J. Chem. Ecol. **23:** 2777–2789.

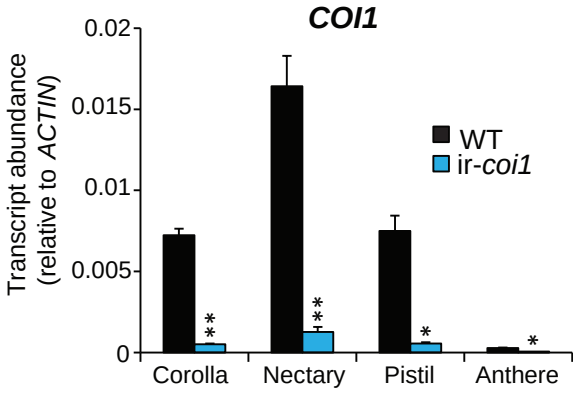

Supplemental Figure 1. *COI1* transcript levels are silenced to similar levels in all floral tissues of ir-*coi1* plants. Transcript abundance (relative to gene expression of *ACTIN*) of *COI1* in individual floral tissues of WT and ir-*coi1* plants on the day before anthesis (mean + SE, n = 3, each replicate was obtained from 20+ pooled tissues of 3 plants). Asterisks represent significant differences between the same floral tissue of WT and ir-*coi1* (unpaired t-test; *, p <0.05; **, p <0.001).

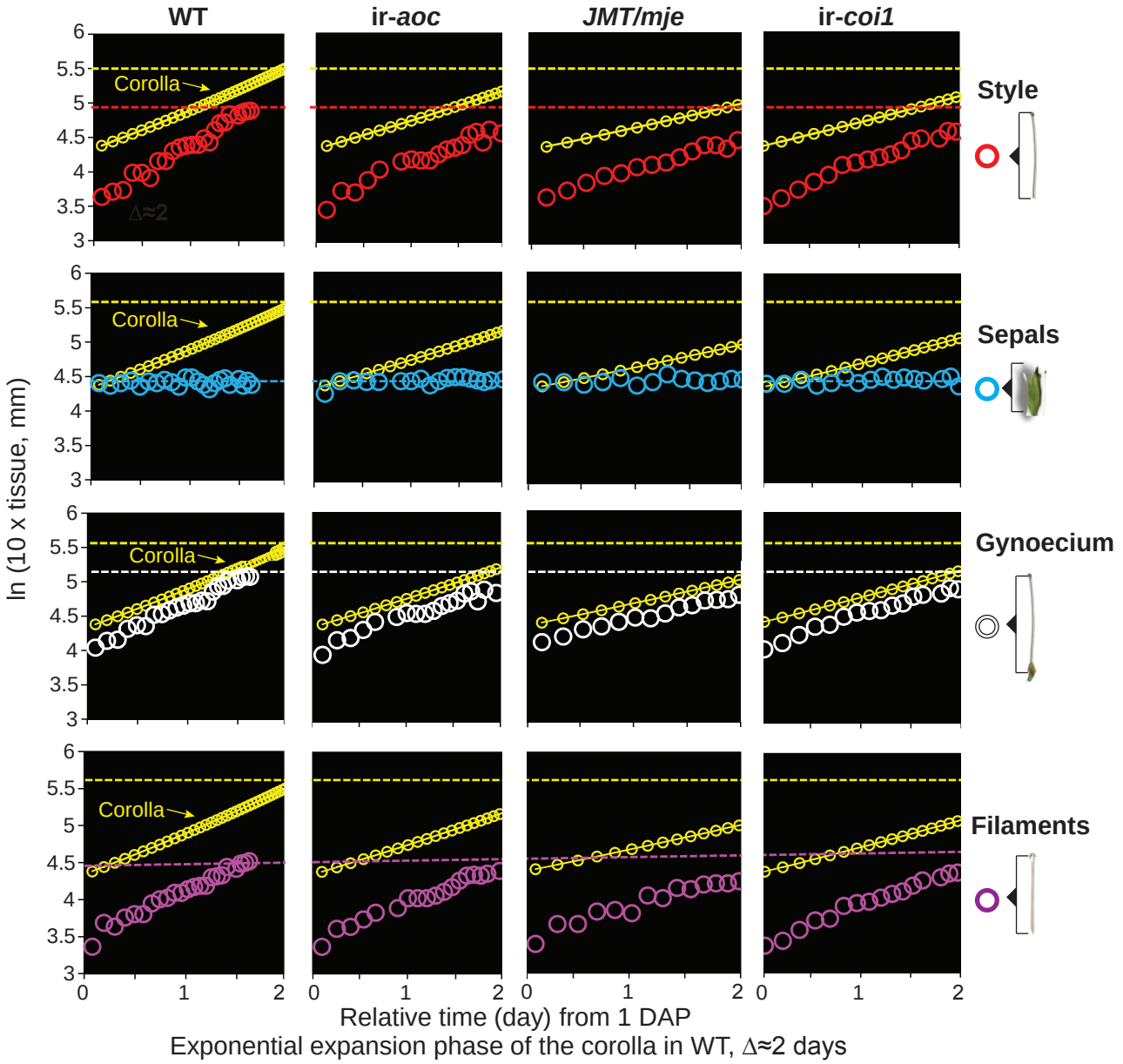

Supplemental Figure 2. The growth rate of different flower organs is altered in JAs biosynthesis/perception-deficient transgenic lines during rapid corolla elongation. Best fits for exponential regressions obtained from ln-transformed corolla size (mm) values were used to calculate relative time from corolla protrusion (expressed in DAP, days after the corolla first protruded the sepals) during the duration of the WT corolla exponential elongation phase (2 DAP) in the different genetic backgrounds. Ln-transformed 10 x tissue size (mm) values measured from individual flowers of the different genotypes were plotted against this relative time difference to model the growth of these tissues during the phase of rapid growth in WT flowers. Except for sepals, the different plots highlight major decreases in the growth rate and outcome sizes (scaled down by ln-transformation) at the end of the measurement time window for the different organs of the transgenic lines compared to those of WT plants. Dashed lines indicate WT floral organ length of corolla (yellow), style (red), sepals (blue), gynoecium (white) and filaments (purple) at the end of WT exponential elongation phase (2 DAP).

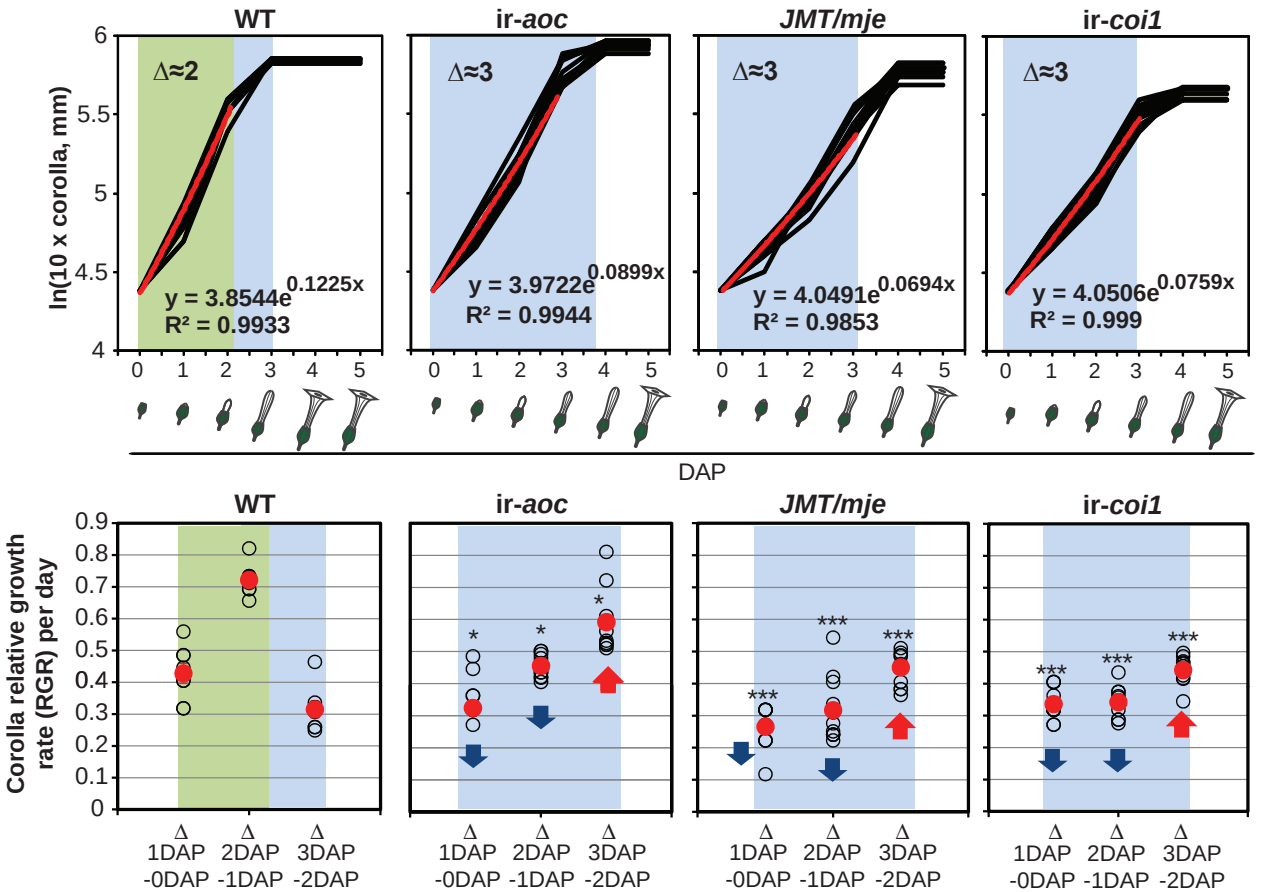

Supplemental Figure 3. Relative growth rate calculations indicate phase-specific effects of JAs signaling deficiency on corolla growth. Corolla length was recorded after dissection from independent flowers collected during the corolla exponential expansion phase of WT flowers (first two days after corolla protrusion, 1 DAP to 3 DAP, range of WT corolla sizes: 8 to 25.3 mm). The duration (Δ in upper panel) of the corolla exponential phase is approximately one day longer in all JAs biosynthesis/perception transgenic plants tested. Best fits for exponential regressions calculated for ln-transformed corolla size (mm) values for each genotype are presented. Corollas' relative growth rates (RGR) per day were calculated according to (Hill and Malmberg, 1991). Asterisks represent significant differences between RGR of WT and transgenic lines at the same DAP (unpaired t-test; *, p <0.05; *** p <0.0001).

Supplemental Data. Stitz et al. Plant Cell (2014) 10.1105/tpc.114.128165

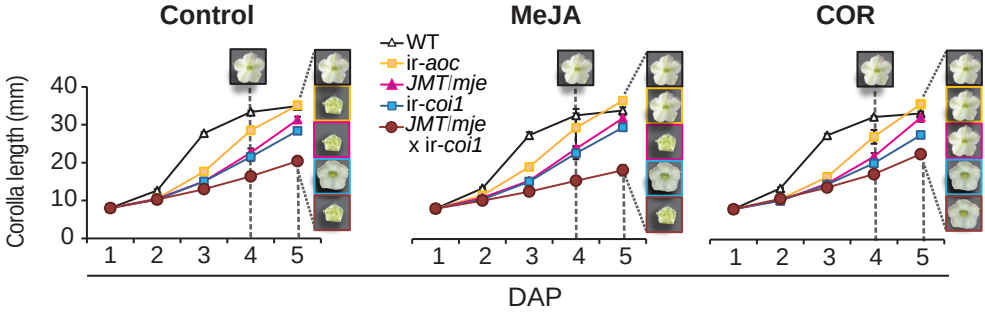

Supplemental Figure 4. Delayed maturation of ir-aoc, JMT/mje, and ir-coi1 cannot be recovered by MeJA or coronatine (COR) treatment. Mean (± SD, n = 5) increase in corolla length in intervals of 1 day from 1 DAP (the day after the corolla protruded the sepals) until anthesis. Plants were treated prior measurements every other day for 10 days with 100 µM MeJA, 1 µM COR or a control solution. Insets indicate days of corolla limb opening.

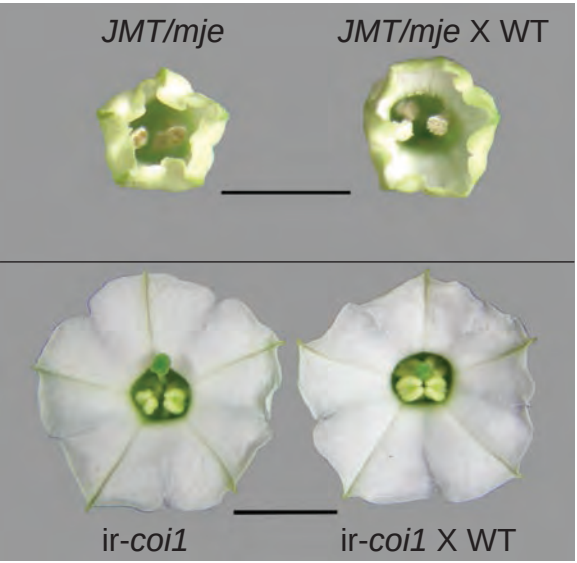

Supplemental Figure 5. Crosses between WT and ir-*coi1* and *JMT*/*mje* plants exhibit corolla phenotypes of their transgenic parents. Flowers of heterozygous plants derived by crosses between WT and *JMT*/*mje* show the characteristic defective limb opening for JAs deficient plants. The back cross with ir-*coi1* shows complete limb opening and the typically un-dehiscing anthers of homozygous ir-*coi1*. Scale bar, 5 mm.

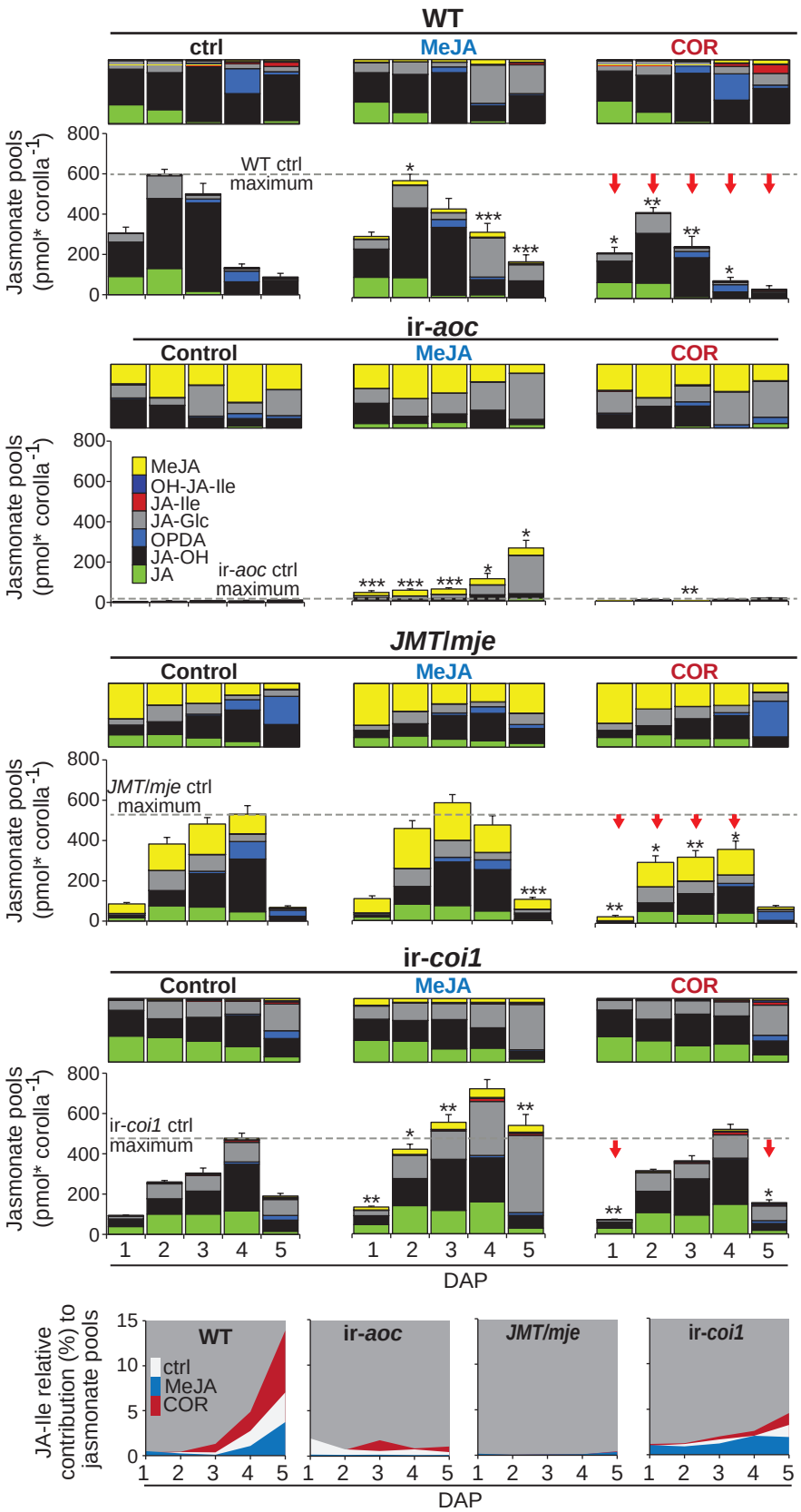

Supplemental Figure 6. COR application reveals a negative feedback effect of JA-Ile signaling on developmentally-regulated JAs pools of corollas. (**A**) Mean (+SE, *n* = 3) summed levels (lower panels) of the seven most abundant JAs (JA, OH-JA, OPDA, JA-Glc, JA-Ile, OH-JA-Ile and MeJA) as detected at the indicate time after protrusion (DAP; days after the corolla first protruded the sepals) in corolla tissues treated either with control, COR and MeJA solutions. JAs were quantified as described in the method section by HPLC-MS/MS analysis. Total JAs were expressed in pmol per corolla to take into account relative differences in genotype water contents. 100% stacked columns above jasmonate pools depict relative contribution of each JAs to the total jasmonate pools of wild type, ir-*aoc*, *JMT*/*mje* and ir-*coi1* corollas (normalized to 100%). Each replicate was obtained from 20+ pooled tissues of 3 plants. Grey dashed lines indicate the maximum levels measured in control corollas for each genotype. Asterisks indicate significant differences between control and MeJA or COR treated tissues of the same genotype and DAP (unpaired t-test; *, p <0.05, ** p <0.001, *** p <0.0001). (**B**) Relative contribution (%) of JA-Ile to jasmonate pools in corollas of control (white), COR (red) or MeJA (blue) treated plants. COR application increases the relative contribution of JA-Ile to the JAs pools.

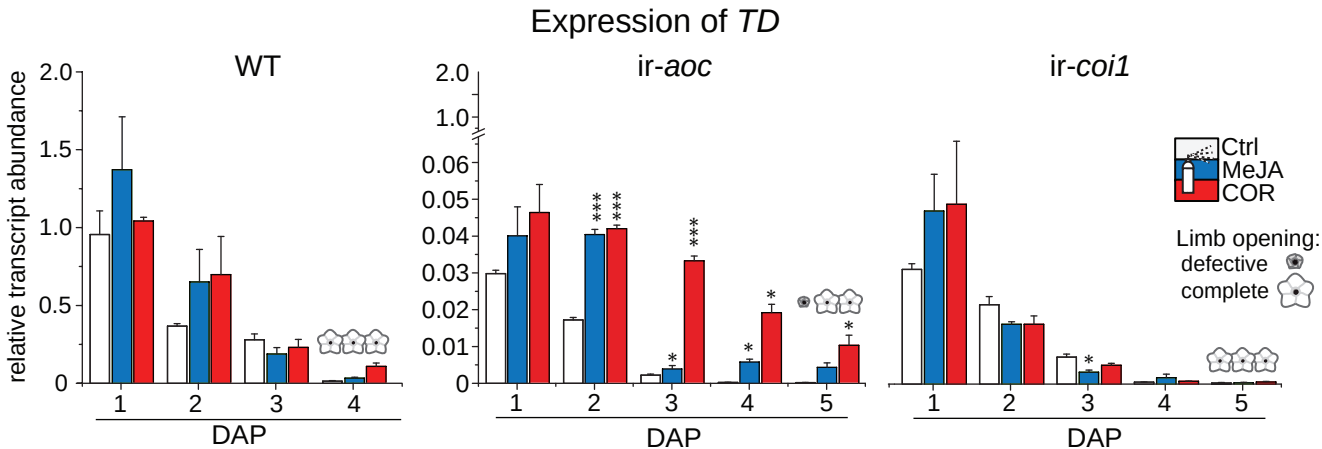

Supplemental Figure 7. Reduced *TD* transcript levels in JAs but not in COI1 deficient corollas are partly rescued by MeJA/COR application. Transcript abundance (relative to *ELONGATION-FACTOR 1ALPHA* (*EF1α*) gene expression) of *THREONINE DEAMINASE* (*TD*) in dissected corolla tissues of WT, ir-*aoc* and ir-*coi1* flowers at indicated day after protrusion (DAP; days after the corolla first protruded the sepals) and treatments (mean + SE, *n* = 3, each replicate was obtained from 20+ pooled tissues of 3 plants). MeJA/COR inhibit the developmental decline in AOC flowers more strongly than those in COI flowers. Asterisks represent significant differences between ctrl and treated tissues of the same genotype and DAP (unpaired t-test; *, $p < 0.05$; *** $p < 0.0001$).

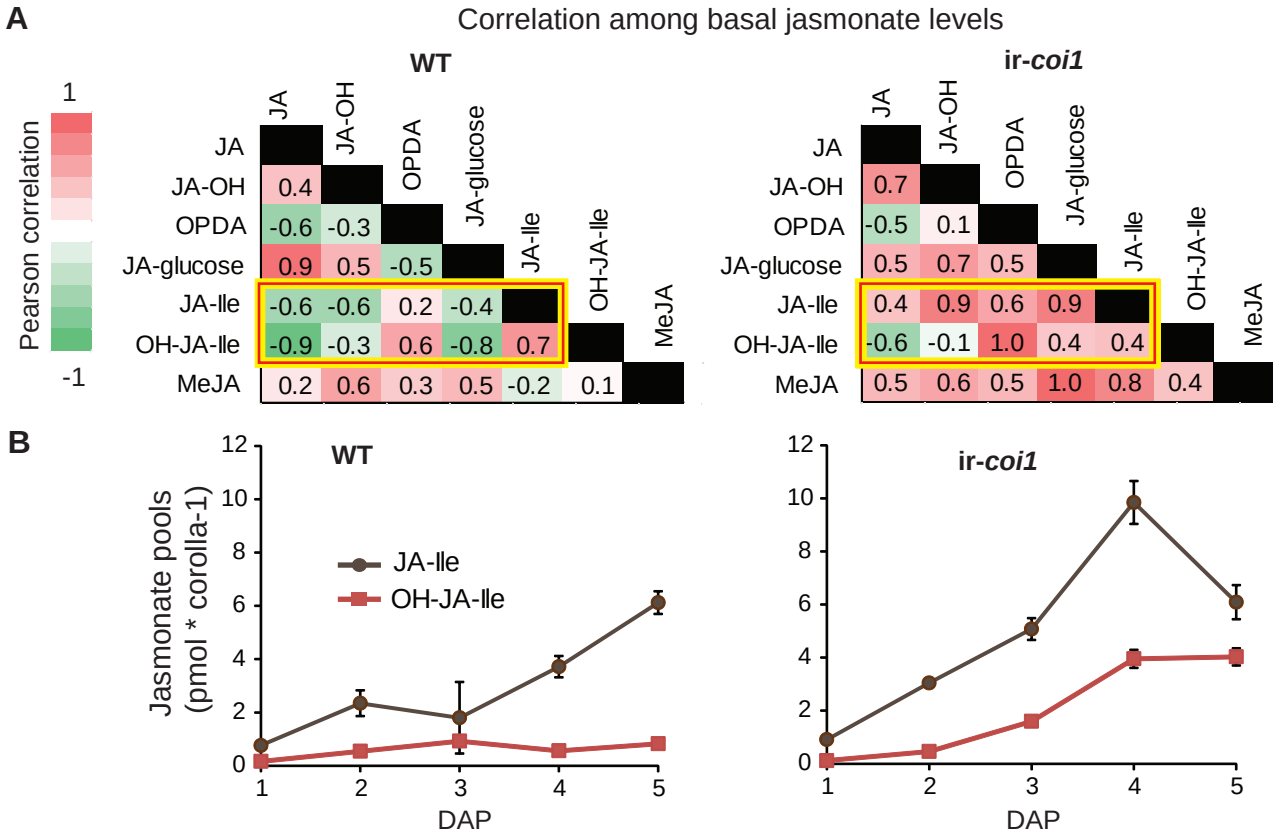

Supplemental Figure 8. Silencing *COI1* expression remodels developmentally regulated effects on JA-Ile accumulation. (A) Correlation matrices for basal JAs levels in untreated corollas of WT and ir-*coi1* plants. Expression vectors obtained for the developmental regulation of JAs levels in WT and ir-*coi1* corollas during the complete time line were used to compute intra-genotype pairwise Pearson correlation coefficients. Significant shifts in the correlation of JA-Ile and its main catabolite (OH-JA-Ile) with other JAs were observed when silencing *coi1*, which is clearly seen in increases in JA-Ile and OH-JA-Ile levels in ir-*coi1* corollas **(B)** Mean (± SE, *n* = 3, each replicate was obtained from 20+ pooled tissues of 3 plants) levels of JA-Ile and its main catabolite OH-JA-Ile in WT and ir-*coi1* corollas, highlighting the feedback control effect of COI1 on the homeostasis of JA-Ile. (DAP; days after the corolla first protruded the sepals).

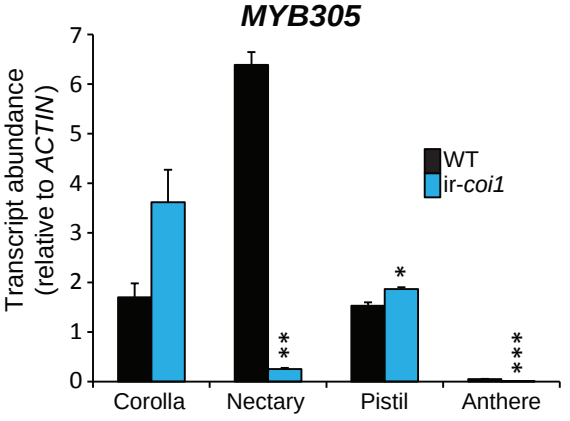

Supplemental Figure 9. Floral expression of *NaMYB305* primarily expressed in nectary tissues is impaired in COI1 deficient nectaries. Transcript abundance (relative to gene expression of *ACTIN*) of *MYB305* in individual floral tissues of WT and ir-*coi1* plants at the day before anthesis (mean + SE, $n = 3$, each replicate was obtained from 8+ pooled tissues of 4 plants). Asterisks represent significant differences between the same floral tissue of WT and ir-*coi1* (unpaired t-test; *, $p < 0.05$; **, $p < 0.001$; **, $p < 0.001$; *** $p < 0.0001$).

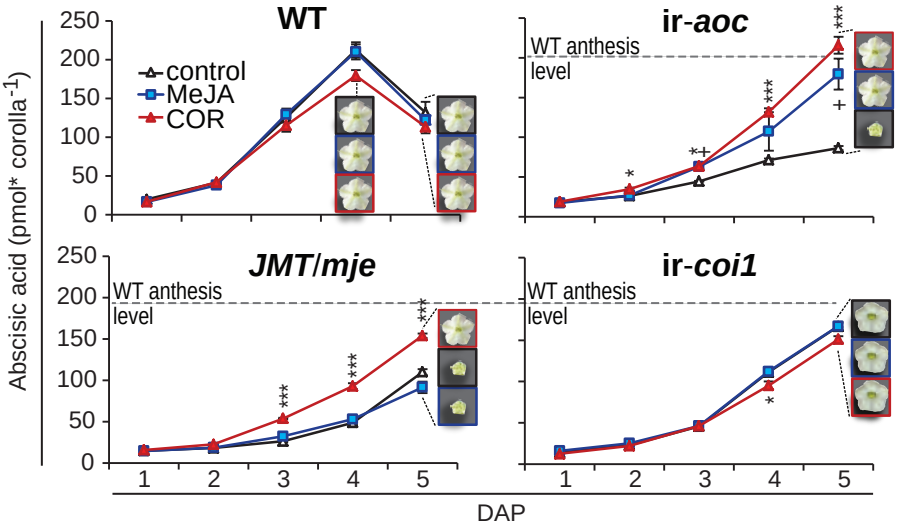

Supplemental Figure 10. Developmentally regulated abscisic acid (ABA) accumulation during corollas expansion involves COR/JA-Ile signaling. Levels of abscisic acid (ABA) as detected at the indicated day after corollas protruded sepals (DAP; days after the corolla first protruded the sepals) in dissected corolla tissues of wild type, ir-*aoc*, *JMT*/*mje* and ir-*coi1* flower buds (Mean ± SE, *n* = 3, each replicate was obtained from 20+ pooled tissues of 3 plants). Flower insets show opening state of flowers at anthesis. Grey dashed lines denote ABA levels of WT flowers at first night of anthesis. Asterisks (COR) and plus signs (MeJA) represent significant differences compared to control treated tissues of the same genotype. (unpaired t-test; */+ p <0.05, **/++ p <0.001, ***/+++ p <0.0001).

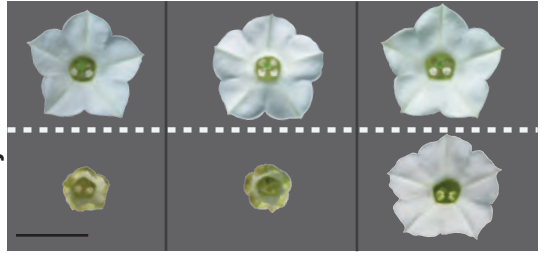

Supplemental Figure 11. ABA treatment does not restore corolla limb opening in JAs deficient flowers. WT and *JMT*/*mje* were treated every other day with 200 µM ABA as described in Ré et al., (2011), 1 µM coronatine (COR) or with a control solution. The opening of flower corollas was monitored one week after initial treatments. Scale bar, 10 mm.

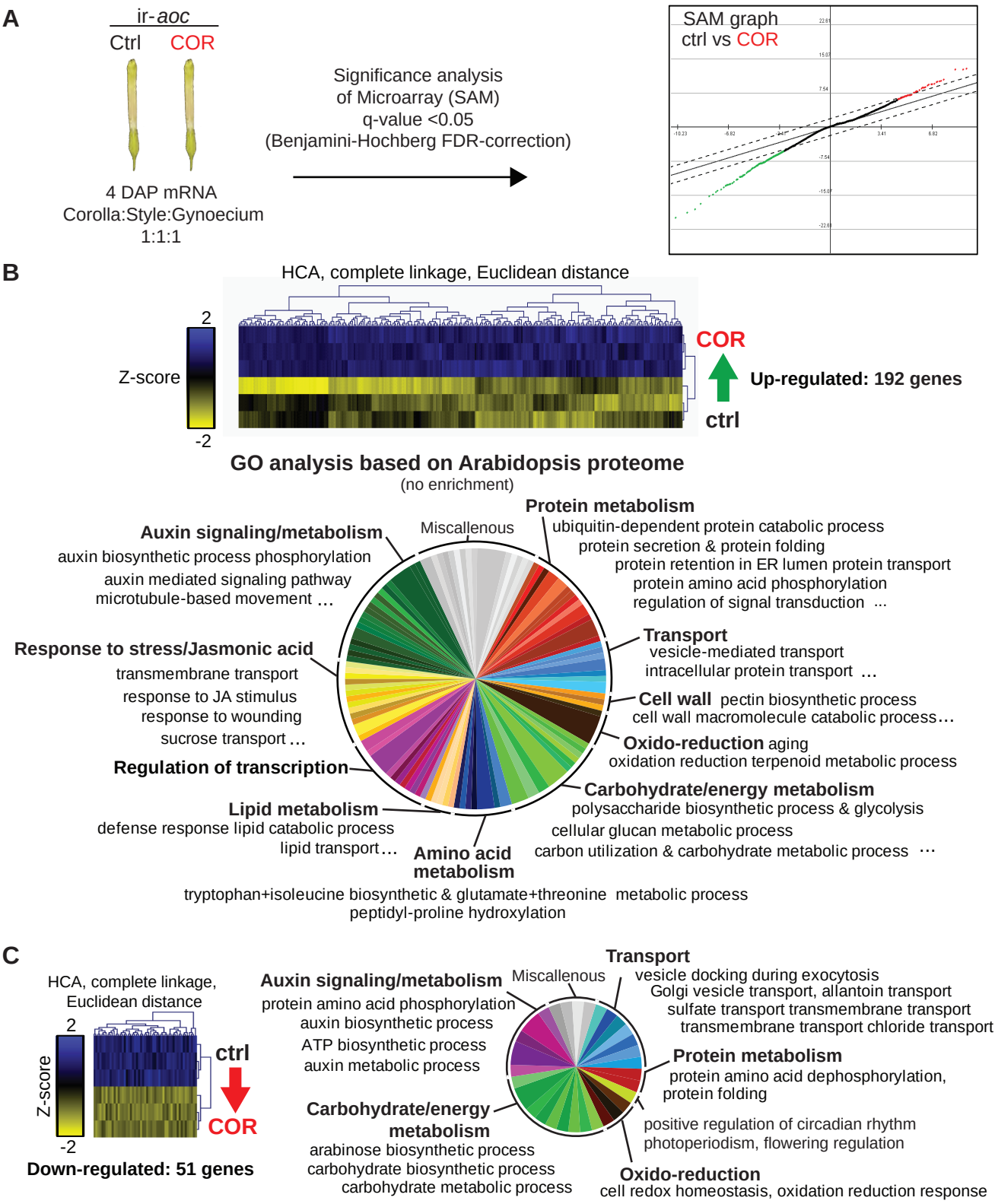

Supplemental Figure 12. Coronatine application on ir-*aoc* flowers activates transcriptomic changes in flower signaling, metabolic and developmental processes. (**A**) Experimental design for sample collection, microarray analysis and statistical analysis. Floral buds at 4 DAP (4 days after corolla protruded and appeared outside sepals) of ir-*aoc* - treated with ctrl (control) or 1µM COR (coronatine) solution - were dissected and 3 biological replicates of each tissue (complete corolla, style and gynoecium tissues) were collected. Individual replicates were obtained from 20+ flowers of each 2 plants. cDNA synthesized from extracted RNA pools were combined with an equal contribution of each tissue types. Microarray data (3 replicates obtained from 3 independently produced pools of cDNA) were 75-percentile normalized and analyzed using significance analysis of microarray (SAM, Benjamini-Hochberg FDR threshold of 5%) for differentially regulated genes between ctrl- and COR-treated flowers **(B,C)** Hierarchical clustering analysis (HCA) on differentially regulated genes and classification of encoded biological processes. Expression vectors for significantly up- (COR>ctrl) **(B)** and down-regulated **(C)** (ctrl>COR) genes were scaled using the Z-score function and aggregated by HCA using the Euclidean distance as clustering metric and the complete linkage method. Gene ontologies (GO) were attributed to differentially regulated probe sets according to best BlastX hits obtained with the Arabidopsis TAIR10 proteome for an e-value threshold of 1e-15. Pie charts depict relative proportions in up- and down-regulated biological processes. Biological processes were arbitrarily grouped as large process groups and examples of the main processes represented in each group are provided. For this Figure, unlike in **Figure S13**, biological process overrepresentation was not tested using hypergeometric tests.

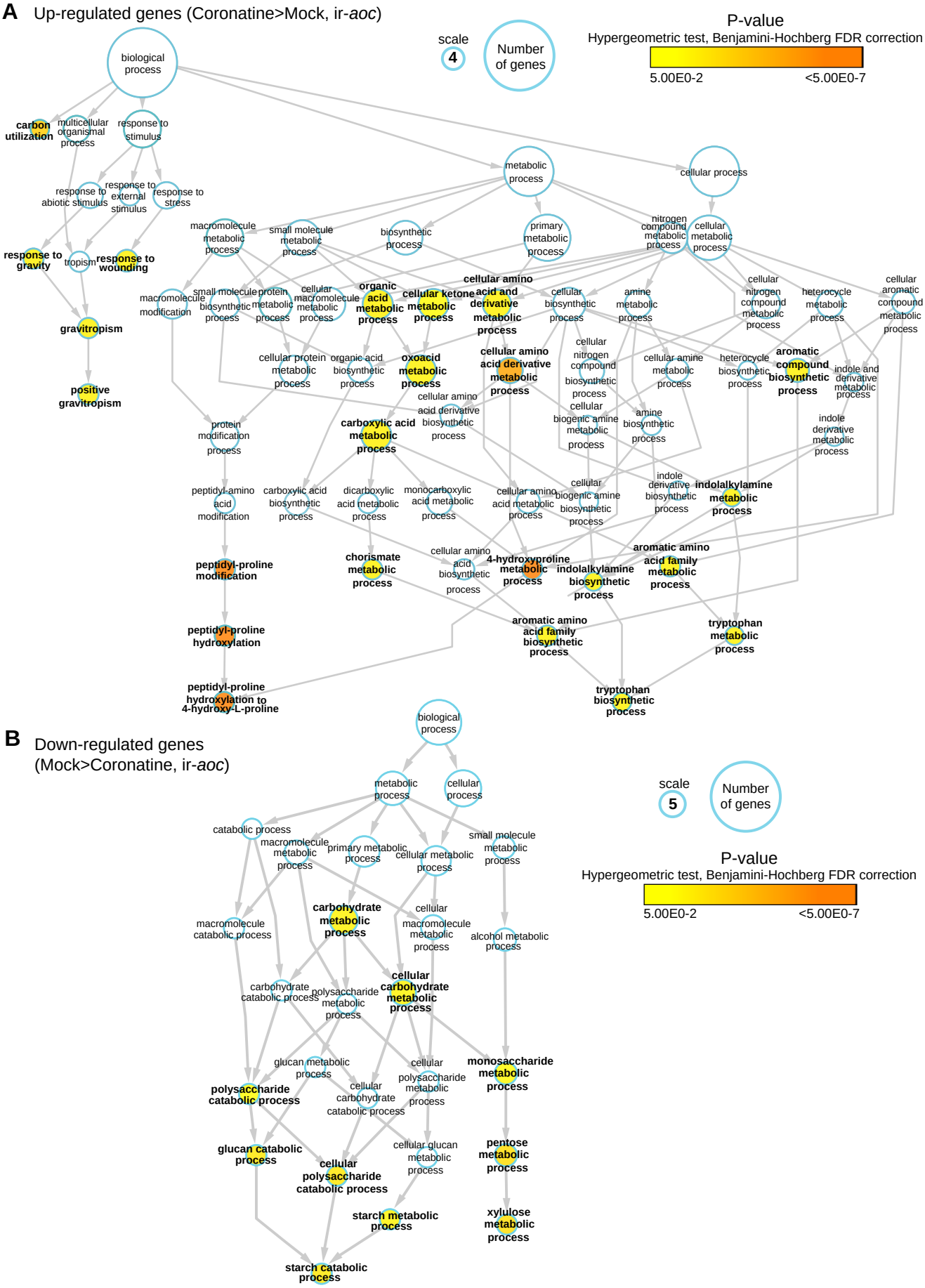

Supplemental Figure 13. BINGO analysis of biological process overrepresentation.

Overrepresentation analysis of ir-*aoc* flower genes significantly up- and down-regulated by the coronatine treatment identifies specific reconfigurations of primary and secondary metabolism transcriptional machineries. Up- and down-regulated genes by the coronatine treatment compared to the control solution and identified by SAM were independently analyzed using the BINGO plugin available for the network visualization software Cytoscape. GO terms were attributed according to best BlastX hits obtained with the Arabidopsis TAIR6 proteome for an e-value threshold of 1e-15. Overrepresentation for particular processes was assessed using hypergeometric tests with a Benjamini-Hochberg FDR correction threshold of 5% versus whole annotated genes. GO networks were constructed using the Cytoscape Hierarchical layout. Node size is proportional to the number of genes associated to a particular GO and node color denotes for the FDR-corrected P-value for a GO relative enrichment.

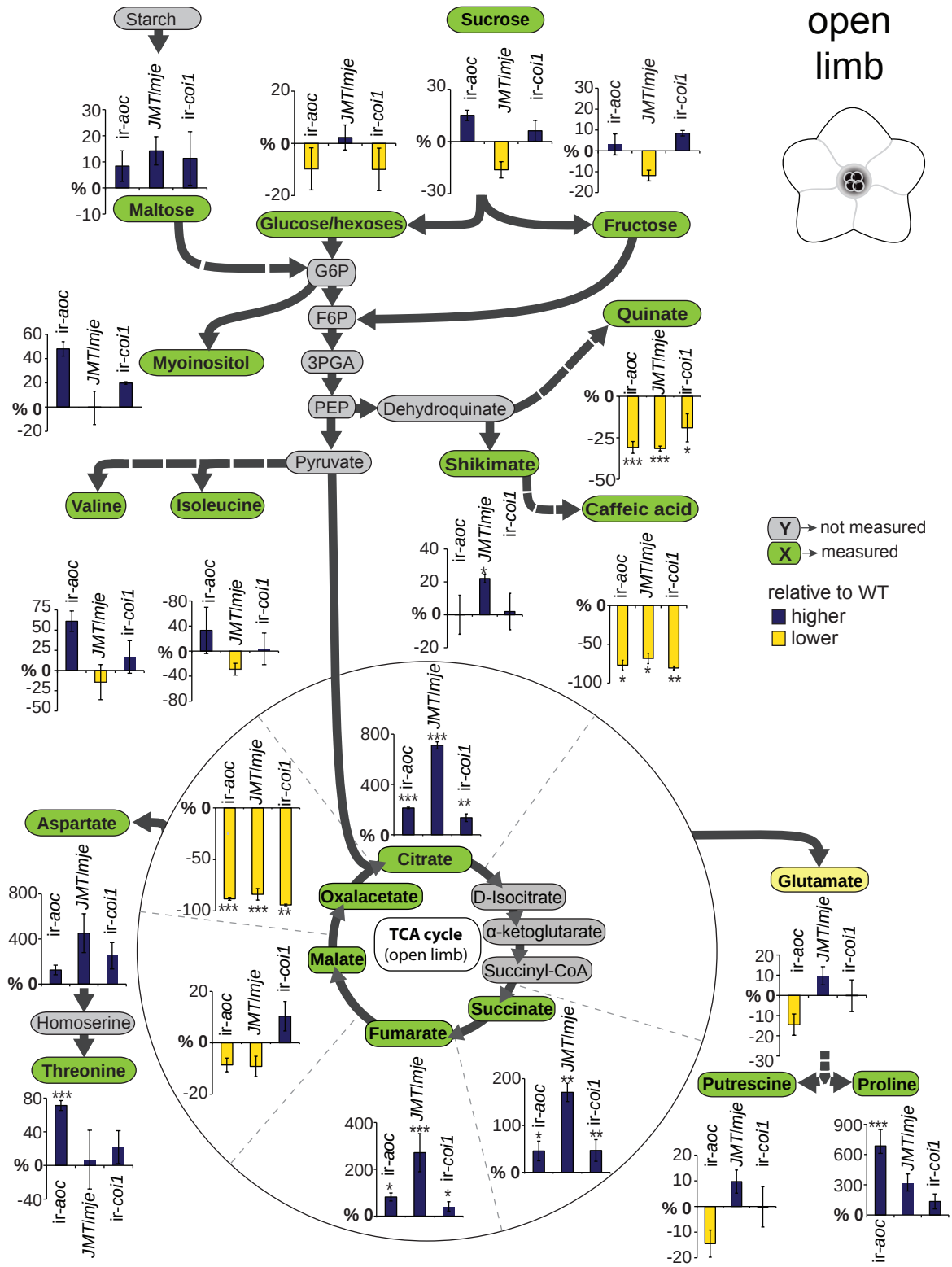

Supplemental Figure 14. Accumulation of carbohydrates and intermediates of energy metabolism in limbs at anthesis is altered in lines with alterations in the JAs-signaling cascade. Relative changes (%) in metabolite accumulation compared to WT as detected in corolla limbs at anthesis of control treated ir-*aoc*, *JMT*/*mje* and ir-*coi1* flowers. Blue bars indicate higher and yellow bars lower level than WT. Asterisks indicate significant differences compared to WT levels (mean + SE, *n* = 3, each replicate was obtained from 20+ pooled tissues of 3 plants). Glucose, combined glucose and hexoses; G6P, glucose 6-phosphate; F6P, fructose 6-phosphate; GADP, glyceraldehyde 3-phosphate; PEP, phosphoenolpyruvate. Derivatized metabolic extracts were analyzed by GCxGC-TOF-MS as described in Gaquerel et al. (2009). Asterisks denote significant differences between limb tissues of WT and corollas tissues of transgenic (unpaired t-test; * p <0.05, ** p <0.001, *** p <0.0001).

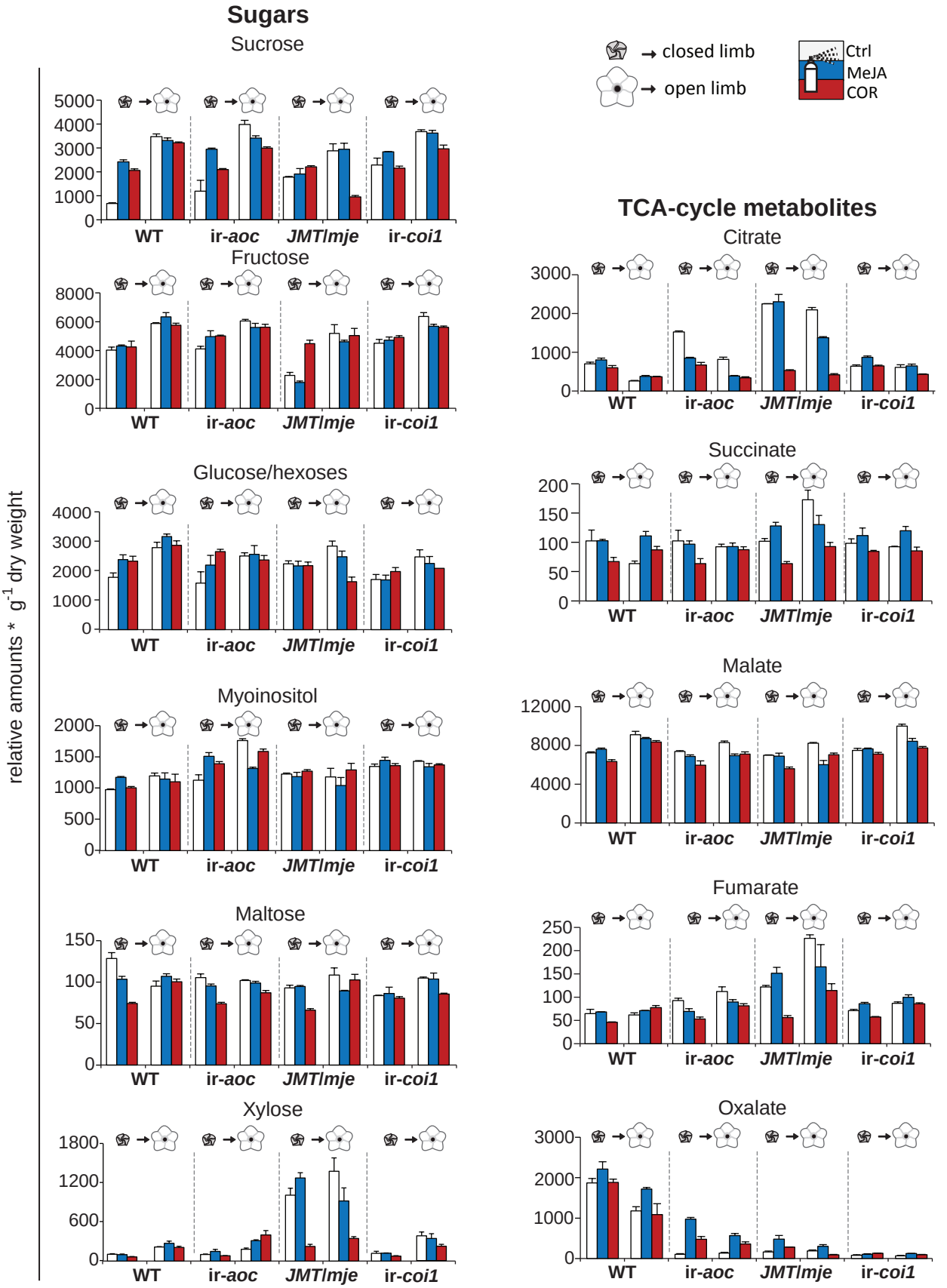

Supplemental Figure 15. Developmental changes in carbohydrate composition and accumulation of intermediates of the TCA cycle during anthesis are regulated via JAs signaling. Metabolite accumulation was monitored in closed and open corolla limbs of WT, ir-*aoc*, *JMT*/*mje* and ir-*coi1* flowers after control (Ctrl/white), methyl jasmonate (MeJA/blue) and coronatine (COR/red) treatment (mean + SE, *n* = 3, each replicate was obtained from 20+ pooled tissues of 3 plants). Glucose, combined glucose and hexoses. Samples were analyzed by GCxGC-TOF-MS as described in Gaquerel et al. (2009).

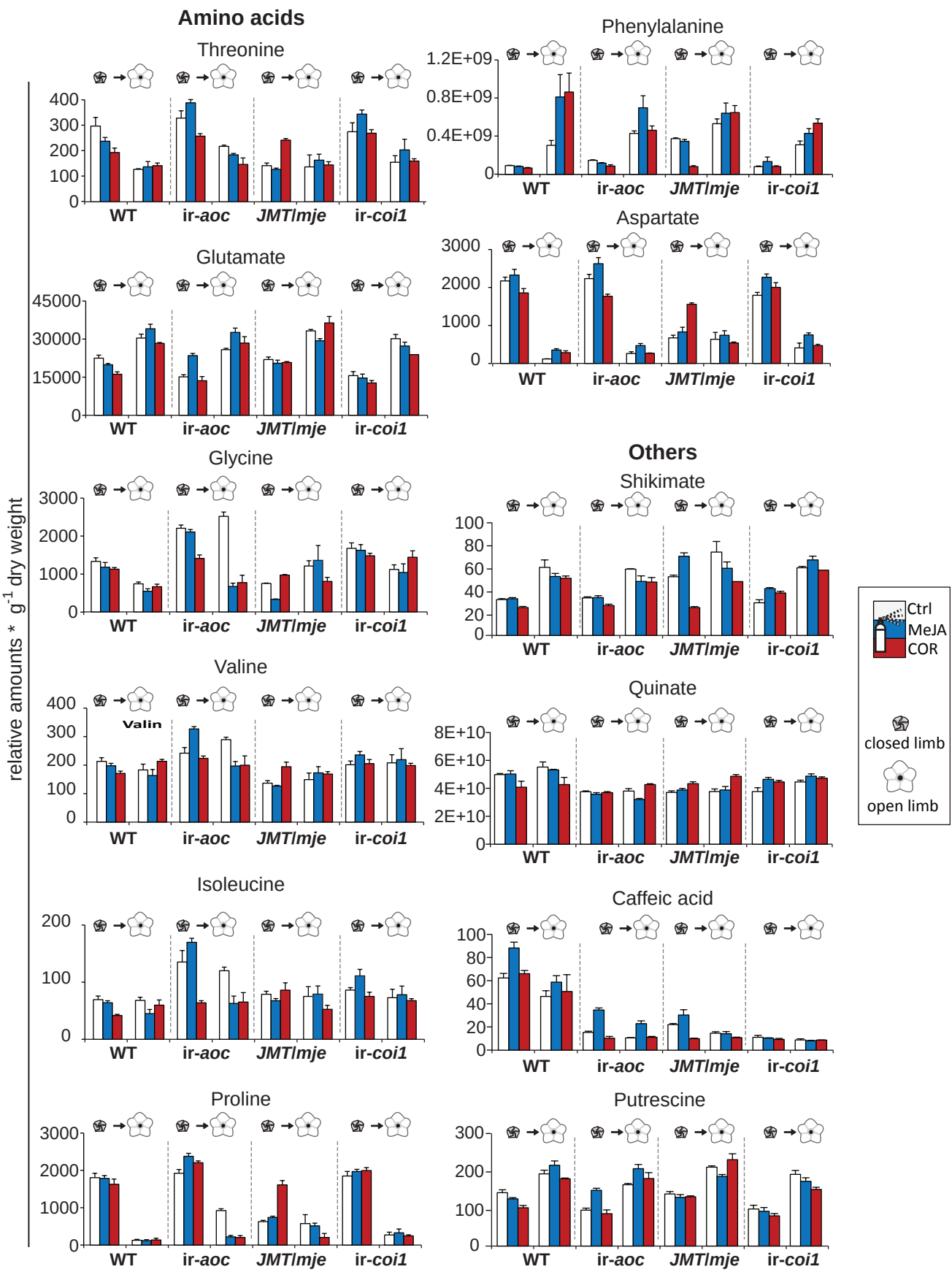

Supplemental Figure 16. Limb accumulation of some amino acids and other metabolites is compromised by JAs deficiency and can be rescued by MeJA or COR applications.
Metabolite accumulation was monitored in closed and open corolla limbs of WT, ir-*aoc*, *JMT*/*mje* and ir-*coi1* flowers after control (Ctrl/white), methyl jasmonate (MeJA/blue) and Coronatine (COR/red) treatment (mean + SE, *n* = 3, each replicate was obtained from 20+ pooled tissues of 3 plants). Samples were analyzed by GCxGC-TOF-MS as described in Gaquerel et al.(2009).

Supplemental Table 1. Sequences of gene-specific primers used for RT-qPCR.

Gene	Forward Primer	Reverse primer
ACTIN	5´-GGTCGTACCACCGGTATTGTG-3´	5´-GTCAAGACGGAGAATGGCATG-3´
AOS	5´-GACGGCAAGAGTTTTCCCAC-3´	5´-TAACCGCCGGTGAGTTCAGT-3´
BAM	5´-ACACAGATCAGTGGGGAAGG -3´	5´-ACAATGGTGTCCCCTAGCAG-3´
CHAL1	5´-TCATTTGGATAGTATGGTCGGG-3´	5´-ACCGTTGATAGCGCCATCGC-3´
COI1	5´-CAGGGCATCTTCAGCTGGTC-3´	5´- CGGGATGCTCAGCAACGA-3´
EF1	5´-CCACACTTCCCACATTGCTGTCA-3´	5´-CGCATGTCCCTCACAG-3´
JAZd	5´-GAGATTGTAGATTCCGGCAAGGTCA-3´	5´-TTCTCAGCTGAATCACCTGA-3´
MYB305	5´-ATGCTAAGTGGGGAAACAG-3´	5´-GCAATTGCATGGACCAGA-3´
NEC1	5´-TGCTGTTTTTGCCGCTCCTT-3´	5´-ACCACATCGTGGCACAGAGAGT-3´
OPR	5´-ATGCCAGATGGAACTCATGCTATTT-3´	5´-TATCAAACTTGCCAAGATTCTGAGC-3´
TD	5´-TAAGGCATTTGATGGGAGGC-3´	5´-TAAGGCATTTGATGGGAGGC-3´